ErbB Signaling Is Required for the Proliferative Actions of GLP-2 in the Murine Gut

BERNARDO YUSTA, DIANNE HOLLAND, JACQUELINE A. KOEHLER, MARLENA MAZIARZ, JENNIFER L. ESTALL, RACHEL HIGGINS, and DANIEL J. DRUCKER

Department of Medicine, Samuel Lunenfeld Research Institute, Mt. Sinai Hospital, University of Toronto, Toronto, Ontario, Canada

BACKGROUND & AIMS: Glucagon-like peptide-2 (GLP-2) is a 33-amino acid peptide hormone secreted by enteroendocrine cells in response to nutrient ingestion. GLP-2 stimulates crypt cell proliferation leading to expansion of the mucosal epithelium; however, the mechanisms transducing the trophic effects of GLP-2 are incompletely understood. **METHODS:** We examined the gene expression profiles and growth-promoting actions of GLP-2 in normal mice in the presence or absence of an inhibitor of ErbB receptor signaling, in *Glp2r*$^{-/-}$ mice and in *Egfr*^{wa2} mice harboring a hypomorphic point mutation in the epidermal growth factor receptor. **RESULTS:** Exogenous GLP-2 administration rapidly induced the expression of a subset of ErbB ligands including amphiregulin, epiregulin, and heparin binding (HB)-epidermal growth factor, in association with induction of immediate early gene expression in the small and large bowel. These actions of GLP-2 required a functional GLP-2 receptor because they were eliminated in *Glp2r*$^{-/-}$ mice. In contrast, insulin-like growth factor-I and keratinocyte growth factor, previously identified mediators of GLP-2 action, had no effect on the expression of these ErbB ligands. The GLP-2-mediated induction of ErbB ligand expression was not metalloproteinase inhibitor sensitive but was significantly diminished in *Egfr*^{wa2} mice and completed abrogated in wild-type mice treated with the pan-ErbB inhibitor CI-1033. Furthermore, the stimulatory actions of GLP-2 on crypt cell proliferation and bowel growth were eliminated in the presence of CI-1033. **CONCLUSIONS: These findings identify the ErbB signaling network as a target for GLP-2 action leading to stimulation of growth factor-dependent signal transduction and bowel growth in vivo.**

The actions of enteroendocrine-derived peptide hormones are classically mediated by specific G-protein-coupled receptors expressed on distant target cell types. However, peptide hormones may also exert their actions indirectly via control of other cell types. For example, glucagon-like peptide-1 (GLP-1) secreted from enteroendocrine L cells interacts with specific GLP-1 receptors on neurons and on pancreatic β-cells to stimulate insulin secretion, which in turn regulates hepatic glucose production and glucose uptake.[1] GLP-1 may also act indirectly on target cells, via GLP-1 receptor (GLP-1R)-dependent transactivation of epidermal growth factor (EGF) receptors (EGFR), to stimulate β-cell proliferation.[2]

Glucagon-like peptide-2 (GLP-2), cosecreted together with GLP-1, acts more proximally on the gut epithelium to promote nutrient absorption, cell proliferation, and survival. GLP-2 exerts its actions through interaction with a specific GLP-2 receptor,[3] a member of the glucagon-secretin receptor superfamily.[4] Activation of the GLP-2R leads to enhanced cyclic AMP formation and engagement of anti-apoptotic pathways.[5,6] Remarkably, however, GLP-2R expression has not been identified on enterocytes or crypt cells; rather, the GLP-2 receptor has been localized to enteric neurons,[7–9] enteroendocrine cells,[8–10] and myofibroblasts,[11] suggesting that the majority of GLP-2 actions on the mucosal epithelium are indirect, through liberation and/or activation of one or more downstream mediators.

Consistent with this hypothesis, GLP-2 requires keratinocyte growth factor (KGF) for growth of the large bowel in mice,[11] whereas the anti-inflammatory actions of GLP-2 in the rat ileum and colon are attenuated following administration of a vasoactive intestinal polypeptide antagonist.[12] Moreover, nitric oxide mediates the rapid GLP-2-dependent stimulation of intestinal blood flow,[13] and GLP-2 enhances expression of endothelial nitric oxide synthase in porcine enteric neurons.[8]

Much less is known about the mechanisms recruited by GLP-2 that lead to stimulation of small bowel growth. Insulin-like growth factor-I (IGF-I), a GLP-2-regulated protein expressed in intestinal myofibroblasts, is required for the intestinotrophic actions of GLP-2 in mice.[14] Nevertheless, although GLP-2 and IGF-I induce an overlapping set of growth-related molecules such as β-catenin, Akt, and c-myc in the murine small bowel,[15] the ability of GLP-2 to induce Akt phosphorylation was preserved in *Igf1*$^{-/-}$ mice.[15] Hence, the actions of GLP-2 on the small bowel are complex, likely involving additional mediators independent of IGF-I. Because GLP-2 and EGF exert overlapping actions encompass-

Abbreviations used in this paper: EGF, epidermal growth factor; EGFR, epidermal growth factor receptor; GLP, glucagon-like peptide; IGF-I, insulin-like growth factor-I; KGF, keratinocyte growth factor.

0016-5085/09/$36.00
doi:10.1053/j.gastro.2009.05.057

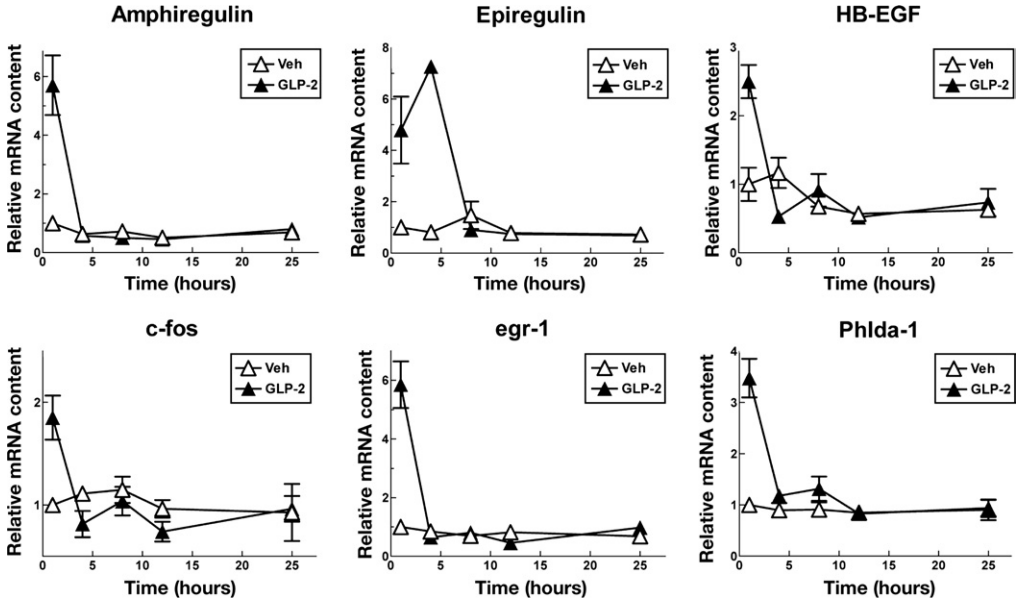

Figure 1. Acute induction of ErbB ligand and IEG transcripts by GLP-2 in mouse jejunum. Levels of mRNA transcripts were determined by real-time quantitative RT-PCR using total RNA isolated from jejunum of CD1 mice killed 1, 4, 8, 12, and 25 hours following a single injection of GLP-2 (0.2 mg/kg) or vehicle alone (PBS). Data, presented as fold induction relative to the vehicle treatment group at time 1 hour, are means ± SE of 2 independent experiments involving a total of 3 mice per condition. SE for data with coefficients of variation ≤ 5% is not visible on the graph.

ing enhancement of nutrient absorption and stimulation of cell proliferation in the gut,[16] we hypothesized that GLP-2 induces its proliferative actions in part through ErbB-dependent pathways. We now report that GLP-2 activates components of the ErbB signaling network and that the trophic actions of exogenous GLP-2 on the murine small bowel are markedly diminished following inhibition of ErbB receptor signaling.

Materials and Methods

Animal Care and Genotyping

Animal studies were carried out in accordance with protocols and guidelines approved by the Animal Care Committees of the University Health Network and Mount Sinai Hospital. Female mice 8–9 weeks of age of the CD1 background were purchased from Charles River Canada (St Constant, Quebec, Canada) or from Taconic (Hudson, NY) and were allowed to acclimatize to the animal facility for 9–10 days before each experiment. *a/a Egfr*^{wa2}/J mice were obtained from The Jackson Laboratory (Bar Harbor, ME), and C57BL/6J-*Glp2r*$^{-/-}$ mice were generated in our laboratory. Heterozygous male and female mice of each strain were crossed to derive the different genotypes utilized in the experiments. Genotyping was performed by polymerase chain reaction (PCR) on tail DNA as previously described.[17,18]

Peptides and Drugs

Human GLP-2 and recombinant mouse EGF were from Bachem (Torrance, CA) and Long-R^3 IGF-I was

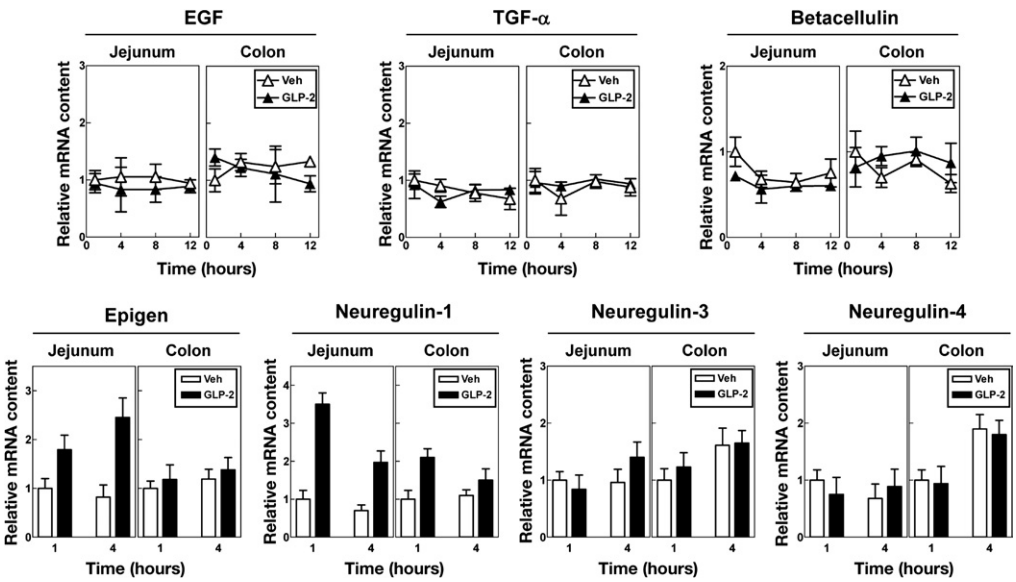

Figure 2. Selective induction of intestinal ErbB ligand transcript expression by GLP-2. Total RNA was isolated from jejunum and colon of CD1 mice at the specified periods of time after a single injection of GLP-2 (0.2 mg/kg) or vehicle (PBS). Levels of mRNA transcripts determined by real-time quantitative RT-PCR are expressed relative to the vehicle values at 1 hour. For EGF, TGF-α, and betacellulin data are means ± SE of 2 independent experiments (3 mice per condition). For the remaining transcripts, data are means ± SE of 4 independent experiments (6 mice per condition).

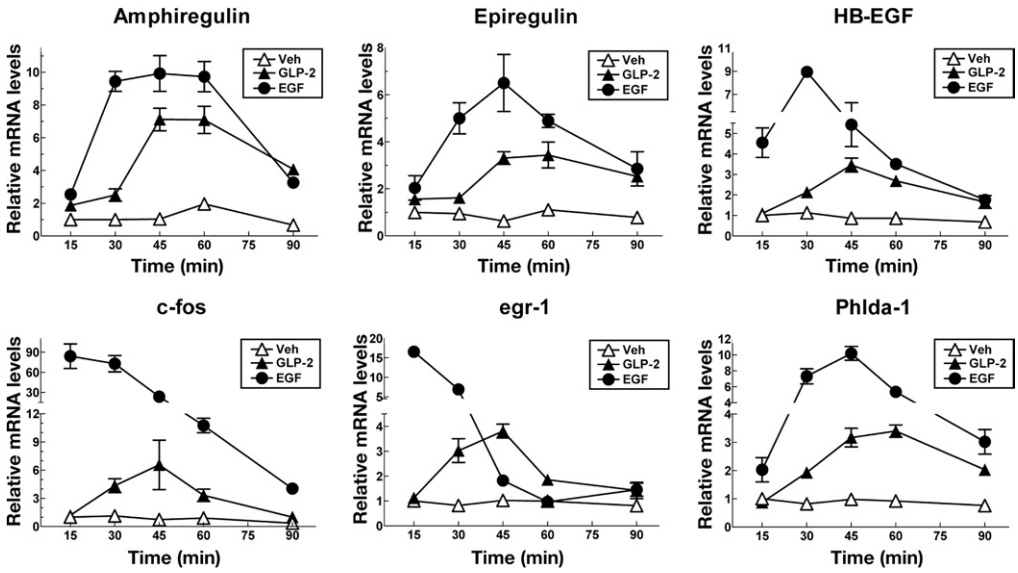

Figure 3. Coordinated induction of specific ErbB ligand and IEG transcripts by GLP-2 and EGF in mouse colon. ErbB ligand and IEG transcript levels were determined by real-time PCR in total RNA from the colon of CD1 mice following treatment with GLP-2 (0.2 mg/kg), EGF (1 mg/kg), or vehicle (PBS) for the indicated time periods. Data, presented as fold induction relative to the values of the vehicle group at time 15 minutes, are means ± SE of 2 independent experiments involving a total of 4 mice per condition. SE for data with coefficients of variation ≤ 5% is not visible on the graph.

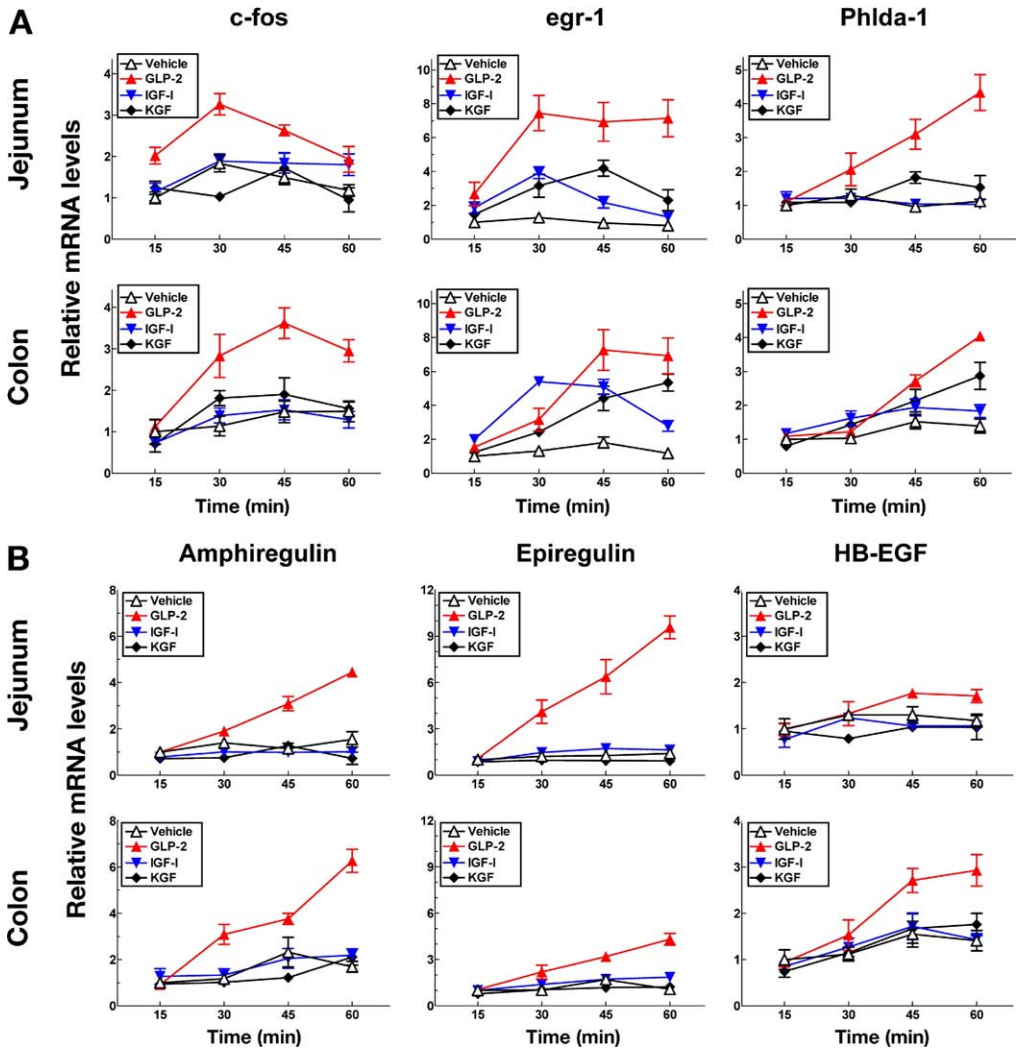

Figure 4. Regulation of specific ErbB ligand and IEG transcript expression by enterotrophic factors in the murine intestine. Total RNA was isolated from jejunum and colon of CD1 mice treated with GLP-2 (0.2 mg/kg), IGF-I (2 mg/kg), KGF (2 mg/kg), or vehicle alone (PBS) for the specified periods of time. mRNA levels of the indicated IEGs (*A*) and ErbB ligands (*B*) were determined by real-time RT-PCR and expressed relative to the vehicle values at 15 minutes. Data are means ± SE of 2 independent experiments involving a total of 4 mice per condition. SE for data with coefficients of variation ≤ 5% is not visible on the graph.

from GroPep Ltd (Adelaide, South Australia, Australia). The DPP-4-resistant analog h[Gly2]GLP-2 was from Pepceutical Ltd (Nottingham, United Kingdom). Human recombinant KGF and the pan-ErbB inhibitor CI-1033 were gifts of Amgen, Inc (Thousand Oaks, CA) and Pfizer Global Research, Inc (Ann Arbor, MI), respectively. The metalloproteinase inhibitor GM6001 was from Chemicon International (Temecula, CA). Peptides were dissolved in phosphate-buffered saline (PBS) and CI-1033 in water, and administered to mice by subcutaneous injection. The 30-mg/kg dose of CI-1033 has previously been demonstrated to suppress constitutive ErbB tyrosine phosphorylation in vivo, in human colon cancer cell tumor xenographs established in nude mice, and also was shown to be well tolerated when given to mice daily for 2–3 weeks.[19,20] GM6001 was given intraperitoneally as a suspension in 4% carboxymethylcellulose (Sigma–Aldrich; Oakville, Ontario, Canada). BrdU (Sigma–Aldrich, 100 mg/kg) dissolved in PBS was injected intraperitoneally to mice 1 hour prior to death.

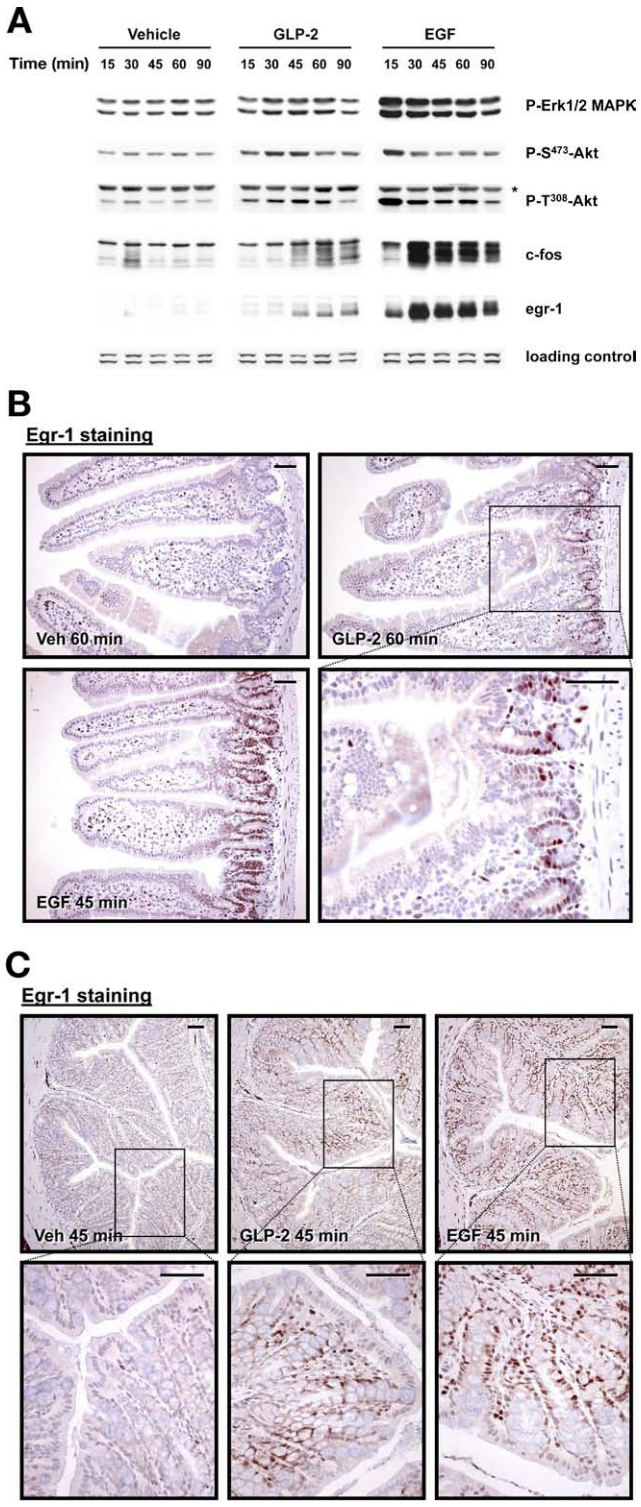

Figure 5. Activation of downstream signaling effectors by GLP-2 and EGF in the mouse intestine. Intestinal tissue samples were collected from CD1 mice killed at the indicated times following GLP-2 (0.2 mg/kg), EGF (1 mg/kg), or vehicle alone (PBS). (*A*) Whole-tissue extracts from colon analyzed by immunoblotting for Erk1/2 MAPK phosphorylated at Thr202 and Tyr204 (P-Erk1/2 MAPK), Akt phosphorylated at Ser473 (P-S^{473}-Akt) or Thr308 (P-T^{308}-Akt), c-fos, and egr-1. Two unidentified proteins cross-reacting with the anti-egr-1 antibody are shown to document loading and transfer conditions (loading control). The *asterisk* denotes an unidentified protein cross-reacting with the anti-phospho-Thr308-Akt antibody. Results are representative of 2 mice per condition and time point. (*B* and *C*). Immunohistochemical detection of egr-1 in transverse cross sections from jejunum (*B*) and colon (*C*) of mice treated with vehicle, GLP-2, or EGF. The areas selected within the *inset boxes* are shown at a higher magnification. Photomicrographs are representative of 3 or 4 mice per group. *Scale bars*, 50 μm.

Tissue Collection and Processing

For experiments involving chronic treatment with peptides, mice were fasted for ~14 hours after the last peptide injection and then killed by CO_2 inhalation. Small intestine and colon were collected and cleaned of mesenteric fat, gently flushed with PBS to remove the fecal material, weighed, and lengths measured after suspending a 1-g weight from their distal end. Adjacent 2-cm intestinal tissue segments were obtained from jejunum (1/4 the small intestinal length distal to the pylorus) and middle portion of the colon. Tissue samples were fixed in 10% neutral-buffered formalin cut into 4 sections and embedded in paraffin or snap-frozen in liquid nitrogen and stored at −70°C. For experiments evaluating acute peptide administration, mice were killed by cervical dislocation, and intestines, and occasionally stomach, were harvested as described above. For comparative purposes, histologic and biochemical analyses were consistently performed on intestinal segments taken from identical anatomic positions.

Intestinal Histomorphometry and Immunohistochemistry

Digital image acquisition was done using a Leica DMR microscope equipped with a Leica DC300F camera and Leica QWin V3 software (Leica Microsystems, Wet-

zlar, Germany). Histomorphometry was performed on 5-μm sections stained with H&E. A minimum of 20 well-oriented villi and crypts from at least 3 different cross sections per intestinal segment and animal were measured to determine villus height and crypt depth. Immunohistochemistry was carried out using indirect immunoperoxidase detection with NovaRED substrate (Vector Laboratories, Burlington, Ontario, Canada) followed by hematoxylin counterstaining. Primary antibodies were used at the dilutions recommended by the manufacturer and included the following: rabbit polyclonal anti-P-Ser473-Akt (Cell Signaling Technology, Beverly, MA), anti-c-fos (Sigma–Aldrich), and anti-egr-1 (Santa Cruz Biotechnology, Santa Cruz, CA; utilized for colon sections), rabbit monoclonal anti-egr-1 (Cell Signaling Technology; used for jejunal sections), and mouse monoclonal anti-BrdU (Invitrogen Canada, Burlington, Ontario, Canada). At least 15 well-oriented jejunal villi and colonic crypts from 3 different cross sections per intestinal segment and mouse were scored to determine the percentage of c-fos-positive nuclei in the mucosal epithelium. BrdU labeling index was assessed in longitudinal sections of crypts containing at least 17 cells, including the Paneth cells. The incidence of BrdU staining for each cell position from the crypt base was scored in a minimum of 100 half crypts from at least 4 different cross sections per intestinal segment and animal. Both the histomorphometric analysis and the immunohistochemic scoring were done in a blinded manner.

Western Blot Analysis

Whole-tissue extracts were prepared by homogenization of intestinal segments in RIPA buffer (1% Nonidet P-40, 0.5% sodium deoxycholate, and 0.1% SDS in PBS) supplemented with protease and phosphatase inhibitors (Sigma–Aldrich), 5 mmol/L sodium fluoride, and 200 μmol/L sodium orthovanadate as described.[21] Rabbit polyclonal antibodies to Akt phosphorylated at Ser473 or Thr308, Erk1/2 MAPK phosphorylated at Thr202 and Tyr204, cleaved caspase-3, Bcl-2, and Bcl-xL were from Cell Signaling Technology and used at a 1:1000 dilution. Rabbit polyclonal antibodies reactive to c-fos, egr-1, ErbB2, and ErbB3 were obtained from Santa Cruz Biotechnology and used at 1:500 dilutions. The rabbit polyclonal anti-EGFR (1:1000 dilution) and the mouse monoclonal anti-HSP90 (1:2000 dilution) antibodies were from Rockland Immunochemicals, Inc (Gilbertsville, PA) and BD Biosciences (Mississauga, Ontario, Canada), respectively.

RNA Isolation and Quantitative Real-Time Reverse-Transcription-PCR

Total RNA from intestinal tissue was extracted by the guanidinium thiocyanate method, and complementary DNA synthesis was performed with random hexam-

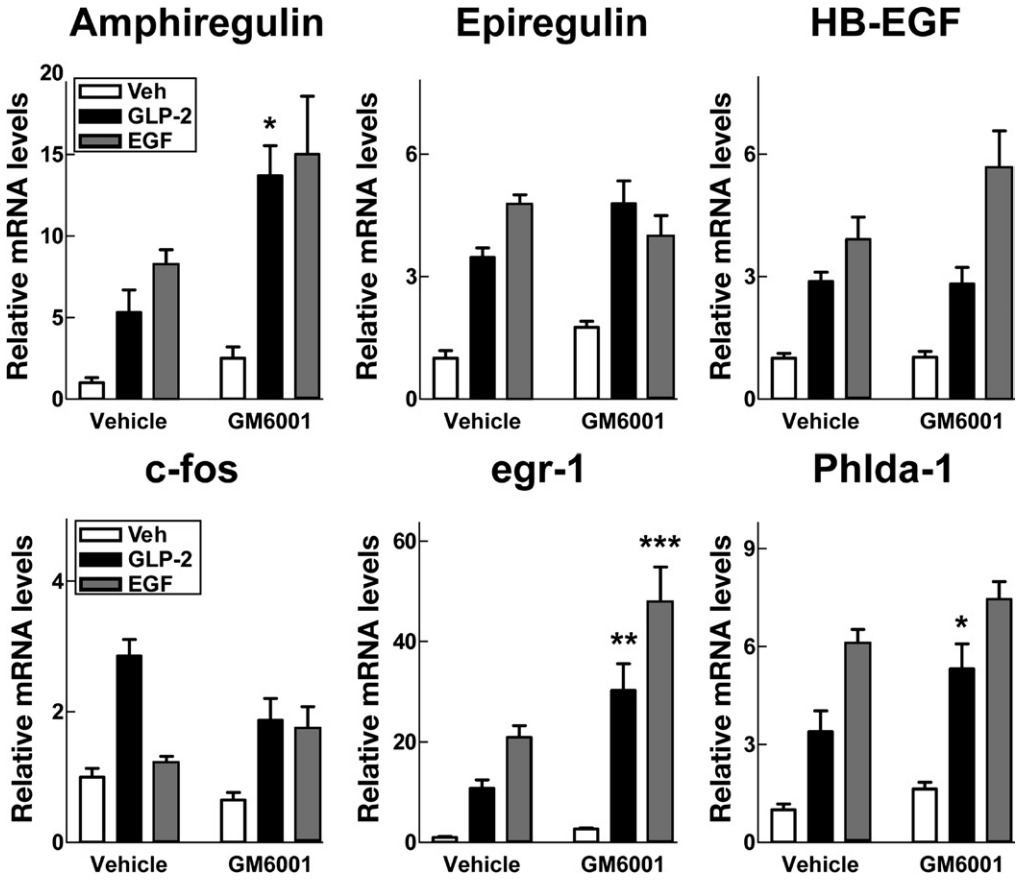

Figure 6. The broad-spectrum metalloproteinase inhibitor GM6001 does not prevent the acute induction of ErbB ligand and IEG transcripts by GLP-2 or EGF in mouse colon. CD1 mice were pretreated with GM6001 (150 mg/kg) or vehicle (4% carboxymethylcellulose in water) and, 40 minutes later, injected with GLP-2 (0.2 mg/kg), EGF (1 mg/kg), or vehicle alone (PBS). Colon samples were collected 45 minutes later, total RNA was isolated, and levels of the indicated transcripts were determined by real-time RT-PCR. Data, expressed relative to the values of vehicle alone-treated mice, are means ± SE of 2 independent experiments (n = 4–6 mice per condition, respectively, in the vehicle- and GM6001-pretreated groups). Two-way ANOVA revealed a $P < .05$ interaction between pretreatment (vehicle, GM6001) and treatment (*vehicle*, *GLP-2*, *EGF*) for c-fos and egr-1. $^{*}P < .05$, $^{**}P < .01$, and $^{***}P < .001$ vs the same treatment within the vehicle-pretreated group.

ers and SuperScript II (Invitrogen). Real-time quantitative PCR was carried out using TaqMan Gene Expression Assays (listed in Supplementary Table 1) and TaqMan Universal PCR Master Mix (Applied Biosystems, Foster City, CA) on an ABI PRISM 7900HT Sequence Detection System (Applied Biosystems). Relative quantification of transcript levels was performed by the $2^{-\Delta Ct}$ method using the threshold cycle (Ct) values obtained from the PCR amplification kinetics with the ABI PRISM SDS 2.1 software (Applied Biosystems). 18S ribosomal RNA (rRNA) was used for normalization since its intestinal expression remained unaltered regardless of the treatment.

Statistical Analysis

Statistical significance was assessed by 1-way or 2-way analysis of variance (ANOVA) followed by the Bonferroni multiple comparison post hoc test by using GraphPad Prism 4 (GraphPad Software Inc, San Diego, CA).

Results

To assess involvement of the ErbB-signaling network in transducing GLP-2 action in the gut, we examined the expression of ErbB family members. GLP-2 rapidly up-regulated levels of messenger RNA (mRNA)

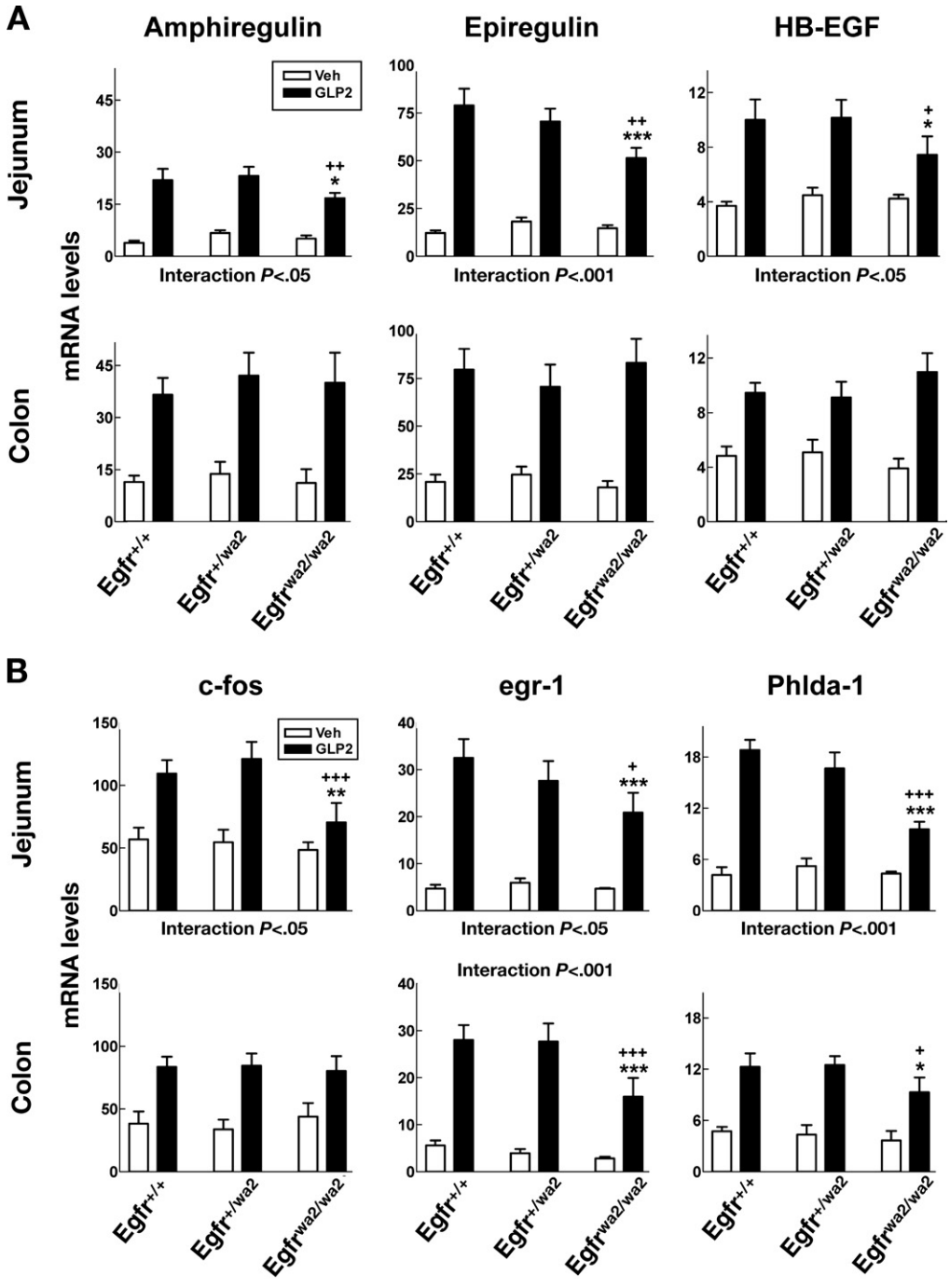

Figure 7. Regulation of specific ErbB ligand and IEG transcript expression by GLP-2 in the *waved-2* mouse intestine. mRNA levels of the indicated ErbB ligands (*A*) and IEGs (*B*) were determined by real-time quantitative RT-PCR in total RNA from jejunum and colon of 14-week-old littermate female mice of the specified *Egfr* genotype, treated for 45 minutes with GLP-2 (0.2 mg/kg) or vehicle alone (PBS). Data are means ± SE of 3 independent experiments, n = 4–6 mice per genotype and condition. Indicated at the bottom of the bar diagrams is the level of significance of the interaction between genotype ($Egfr^{wa2/wa2}$, $Egfr^{+/wa2}$, $Egfr^{+/+}$) and treatment (*vehicle*, *GLP-2*) determined by 2-way ANOVA. $^{*}P < .05$, $^{**}P < .01$, and $^{***}P < .001$ vs GLP-2-treated $Egfr^{+/+}$ mice; $^{+}P < .05$, $^{++}P < .01$, and $^{+++}P < .001$ vs GLP-2-treated $Egfr^{+/wa}$ mice.

encoding the ErbB ligands amphiregulin, epiregulin, and heparin binding (HB)-EGF and their downstream immediate early gene (IEG) transcriptional targets c-fos, egr-1, and Phlda-1 in the jejunum (Figure 1) and colon (Supplementary Figure 1) but not in the stomach (Supplementary Figure 2). Furthermore, the actions of GLP-2 to induce ErbB ligands and IEG expression required the GLP-2 receptor because they were not detected in *Glp2r*$^{-/-}$ mice (Supplementary Figure 3), which exhibited ErbB ligand and receptor expression levels similar to those of Glp2r$^{+/+}$ mice (Supplementary Figure 4). The induction of ErbB ligand genes was selective because GLP-2 had no effect on expression of EGF, transforming growth factor (TGF)-α, betacellulin, neuregulin-3 (Nrg-3), or Nrg-4 in the murine gut (Figure 2). In contrast, Nrg-1 was up-regulated in jejunum and colon within 1

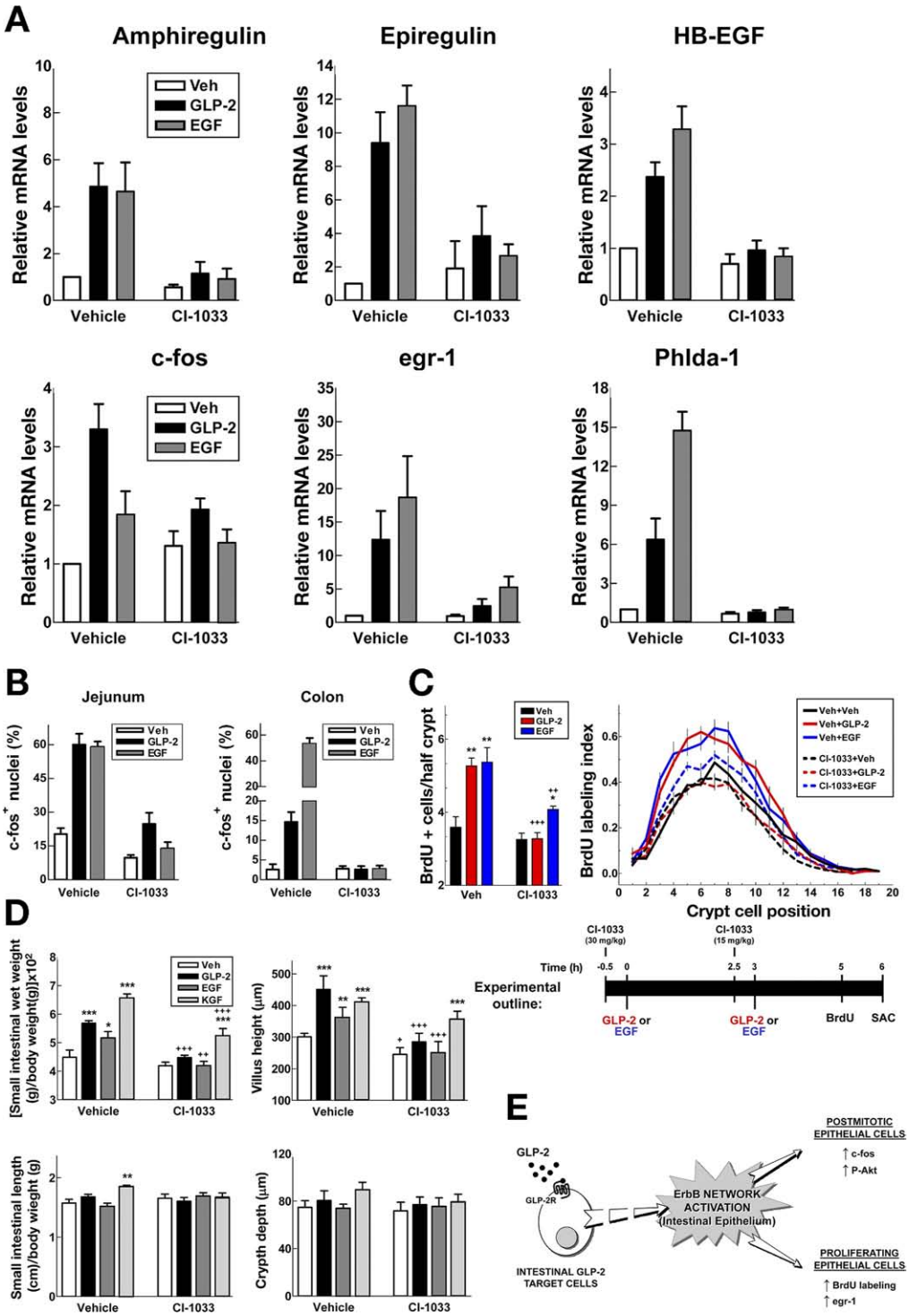

hour of GLP-2 treatment (Figure 2). Moreover, GLP-2 induced expression of epigen in jejunum but not in colon (Figure 2). The specificity of the intestinal response to GLP-2 was further illustrated by the observation that GLP-2 had no significant effect on levels of intestinal mRNA transcripts for KGF, TGF-β1, TGF-β2, TGF-β3, IGF-I, IGF-II, neurotensin, Vegfa, proglucagon, Tff3, inhibin α, or inhibin βA (Supplementary Figure 5, and data not shown).

We next ascertained whether the profile of changes in gene expression and the activity of signaling intermediaries activated by GLP-2 would be similar to that induced by a cognate ErbB ligand. As shown in Figure 3, both GLP-2 and EGF rapidly induced the expression of mRNA transcripts encoding amphiregulin, epiregulin, HB-EGF, c-fos, egr-1, and Phlda-1 in the colon. However, the kinetics of induction were faster and the magnitude of induction was greater following EGF administration. Similar results were observed for EGF and GLP-2 in the jejunum (Supplementary Figure 6).

Because KGF and IGF-I have been proposed as mediators of GLP-2 action,[11,14] we assessed whether these growth factors reproduced the changes in ErbB ligand and IEG gene expression detected following GLP-2 administration. Exogenous KGF and IGF-I transiently upregulated some IEG mRNAs, particularly egr-1, in the gut; however, the inductive effect of GLP-2 was more rapid and robust relative to IGF-I or KGF (Figure 4*A*). In contrast to GLP-2, neither KGF nor IGF-I induced the expression of amphiregulin, epiregulin, and HB-EGF (Figure 4*B*). Hence, the induction of specific ErbB ligand mRNAs constitutes a signature shared by GLP-2 and EGF in the murine intestine.

We next assessed whether GLP-2 regulated signaling molecules activated by the ErbB network. GLP-2 increased levels of active Akt phosphorylated at Ser473 and Thr308 and of c-fos and egr-1 but only modestly stimulated Erk1/2 MAP kinase phosphorylation; the magnitude of induction was relatively greater and more rapid for EGF compared with GLP-2 (Figure 5*A*). The cellular localization of activated phospho-Ser473-Akt, c-fos, and egr-1 was assessed by immunohistochemistry. GLP-2 stimulated Akt phosphorylation in the jejunal and colonic mucosa (Supplementary Figure 7), mainly within the epithelium. However, EGF, but not GLP-2, activated Akt in the colonic outer longitudinal muscle layer (Supplementary Figure 7*B*). Both GLP-2 and EGF induced c-fos (Supplementary Figures 8 and 9) and egr-1 (Figure 5*B* and *C*) nuclear positivity within the jejunal and colonic mucosal epithelium. In the jejunum, GLP-2- and EGF-induced nuclear egr-1 was confined to the crypt epithelium (Figure 5*B*). Following GLP-2 administration, 24% of the jejunal crypt cells showed positive nuclear egr-1 staining; 85% of the egr-1-positive nuclei were located at positions 3–11 within the crypt compartment. In contrast, EGF induced nuclear egr-1 expression more broadly within the entire jejunal crypt epithelium. No significant changes in the expression of multiple apoptosis modulators or in caspase-3 cleavage were observed in the jejunum of normal mice following GLP-2 administration (Supplementary Figure 10).

To determine whether ErbB ligand ectodomain shedding is required for GLP-2-mediated activation of ErbB signaling, we used the broad-spectrum metalloproteinase inhibitor GM6001. Consistent with previous studies,[22,23] GM6001 effectively suppressed (by 85%, $P < .001$, ANOVA) the increase in plasma tumor necrosis factor (TNF)-α elicited by a D-Gal/LPS challenge (Supplementary Figure 11) but failed to attenuate the acute induction of specific ErbB ligand and IEG mRNAs by GLP-2 or EGF in both colon (Figure 6) and jejunum (Supplementary Figure 12). These observations suggest that GLP-2-mediated activation of ErbB network pathways in the murine gut occurs independently of metalloproteinase activity.

Figure 8. Pan-ErbB receptor activity is required for the actions of GLP-2 and EGF in the murine intestine. (*A* and *B*) CD1 mice were pretreated with CI-1033 (30 mg/kg) or vehicle (water) and 30 minutes after injected with GLP-2 (0.2 mg/kg), EGF (1 mg/kg), or vehicle alone (PBS). Intestinal tissue samples were collected 45 minutes later for RNA and c-fos immunohistochemical analyses. (*A*) Jejunal mRNA levels of the indicated transcripts are expressed relative to the values of vehicle-treated mice. (*B*) Percentage of c-fos+ nuclei in the top half of the jejunal villi and in colonic crypts. For *A* and *B*, data are means ± SE of 2 independent experiments involving a total of 3 or 4 mice per condition. (*C*) BrdU labeling in the jejunal crypt compartment of CD1 mice after 2 injections (3 hours apart) of h[Gly2]GLP-2 (0.2 mg/kg), EGF (0.7 mg/kg), or vehicle alone (PBS) with or without pretreatment with CI-1033 (30 mg/kg the first injection and 15 mg/kg the second injection) or vehicle (water) as summarized in the *experimental outline*. Tissue sections were scored for total number of BrdU+ cells per half crypt (*left panel*) and incidence of staining (BrdU labeling index) at each cell position within the crypt (*right panel*). Position 1 corresponds to the base of the crypt. Data are means ± SE (n = 4 mice per condition). *Left panel:* $^{*}P < .05$ and $^{**}P < .01$ vs the corresponding vehicle-treated group; $^{++}P < .01$ and $^{+++}P < .001$ vs the same treatment within the vehicle-pretreated group. *Right panel:* crypt cell positions 3–6, $P < .001$, and 7–10, $P < .05$ for Veh+GLP-2 vs Veh+Veh; crypt cell positions 3–6, $P < .001$, and 7–9, $P < .01$ for Veh+EGF vs Veh+Veh. (*D*) Relative small intestinal weight and length and jejunal histomorphometry in CD1 mice pretreated with vehicle (water) or CI-1033 (30 mg/kg) 30 minutes prior to administration of h[Gly2]GLP-2 (0.2 mg/kg), EGF (0.4 mg/kg), KGF (2 mg/kg), or vehicle alone (PBS) once a day for 9 days. Villus height and crypt depth were assessed on histologic jejunal transverse cross sections stained with H&E. Data are means ± SE of 2 independent experiments (5 or 6 mice per condition). $^{*}P < .05$, $^{**}P < .01$, and $^{***}P < .001$ vs the corresponding vehicle-treated group; $^{+}P < .05$, $^{++}P < .01$, and $^{+++}P < .001$ vs the same treatment within the vehicle-pretreated group. (*E*) Model for the ErbB network as a mediator of GLP-2 action in the murine intestinal mucosa. GLP-2 receptor activation, via a mechanism insensitive to GM6001, engages ErbB-dependent signaling pathways, as exemplified by the up-regulation of ErbB ligand and IEG expression, leading to stimulation of cell division within the crypt compartment and, ultimately, intestinal mucosal growth.

Waved-2 (*wa2*) mice are homozygous for the $Egfr^{wa2}$ allele which encodes a mutant ErbB1 protein with 10%–20% of the normal kinase activity.[18] To ascertain whether GLP-2 engages the ErbB network via ErbB1 (the EGF receptor), we assessed the intestinal gene expression response to GLP-2 in *waved-2* mice. The magnitude of the inductive gene expression response to GLP-2 for amphiregulin, epiregulin, HB-EGF, c-fos, egr-1, and Phlda-1 was significantly diminished in the jejunum, in age- and sex-matched $Egfr^{wa2/wa2}$ mice (Figure 7*A* and *B*). However, only the induction of egr-1 and Phlda-1 was reduced in the colon of $Egfr^{wa2/wa2}$ mice (Figure 7*B*). The reduced GLP-2 response in $Egfr^{wa2/wa2}$ mice was not due to differences in GLP-2R expression (data not shown). In contrast, the trophic response to exogenous GLP-2 was preserved in the small bowel of *waved-2* mice (Supplementary Figure 13).

The studies in *waved-2* mice demonstrate that, although ErbB1 activity transduces a component of the acute jejunal gene expression response to GLP-2, a fully functional *Egfr* locus is not required for the intestinal growth response to exogenous GLP-2. Accordingly, we used an irreversible pan-ErbB receptor tyrosine kinase inhibitor, CI-1033,[19,20] to block signal transduction through all 4 members of the ErbB family. Pretreatment of mice with CI-1033 prevented the GLP-2- and EGF-mediated up-regulation of IEG and ErbB ligand mRNA transcripts in the jejunum (Figure 8*A*). Furthermore, immunohistochemical analysis demonstrated that CI-1033 inhibited the acute induction of nuclear c-fos immunoreactivity by either GLP-2 or EGF in the mucosal epithelium of both jejunum and colon (Figure 8*B*).

We next compared cell cycle progression in the jejunal crypt compartment of mice administered GLP-2 with or without CI-1033 pretreatment. GLP-2 significantly increased the number of cells in S-phase in jejunal crypts either when assessed by crypt position (positions 3–6, $P < .001$, and 7–10, $P < .05$, ANOVA) or by total number of BrdU-positive cells per hemi-crypt (Figure 8*C*). CI-1033 alone did not modify the crypt BrdU labeling index. However, administration of CI-1033 prior to GLP-2 completely inhibited the stimulatory effect of GLP-2 on crypt cell cycle progression. Consistent with the emerging relationship between actions of GLP-2 and EGF, the cellular localization of EGF-stimulated BrdU labeling occurred in positions within the crypt compartment (positions 3–6, $P < .001$, and 7–9, $P < .01$, ANOVA) overlapping those induced following GLP-2 administration (Figure 8*C*). These observations suggest that GLP-2, like the ErbB ligand EGF, increases the rate of cell division in the small intestinal crypt in an ErbB receptor activity-dependent manner.

To determine whether ErbB signaling was required for GLP-2-induced intestinal growth, mice were treated with growth factors, and vehicle or CI-1033 for 9 days. Small bowel mass and jejunal villus height increased significantly after treatment with GLP-2, EGF, and KGF (Figure 8*D*); however, the trophic effects of GLP-2 and EGF were completely abrogated following CI-1033 administration to mice. In contrast, the ability of KGF to stimulate both small intestinal weight and jejunal villus height was preserved in CI-1033-pretreated mice, illustrating the specificity of the pan-ErbB inhibitor. Both GLP-2 and KGF increased colonic growth; however, the trophic effect of KGF, but not GLP-2, remained detectable in the presence of CI-1033 (Supplementary Figure 14). Taken together, these findings implicate an essential role for ErbB signaling in the intestinal trophic response to exogenous GLP-2.

Discussion

The intestinal mucosa of the gut is a dynamic model of cell renewal because the entire mucosal epithelium turns over rapidly within 4 to 6 days in most mammalian species. The control of gut mucosal growth is complex and dependent on multiple inputs from a broad variety of signaling molecules. Insulin-like growth factors, growth hormone, keratinocyte growth factor, hepatocyte growth factor, and fibroblast growth factors have been shown to induce mucosal epithelial proliferation in the small bowel and facilitate mucosal adaptation in preclinical models of intestinal injury. Similarly, peptide hormones, exemplified by peptide YY, glicentin, neurotensin, and GLP-2 activate signaling networks in the gut that promote cell proliferation and restoration of mucosal integrity following experimental gut injury. Nevertheless, the majority of these growth factors and peptide hormones do not appear to be essential for gut growth, as deduced from experiments using chemical inhibitors or gene knockout studies.

The ErbB-signaling network is composed of multiple ligands, including EGF, betacellulin, epigen, TGF-α, epiregulin, amphiregulin, and HB-EGF.[24] These ligands promote autophosphorylation of EGFR/ErbB and activation of well-defined downstream kinase networks. Moreover, the majority of these ligands is produced in the gastrointestinal tract, and gene targeting studies in mice reveal that many ErbB ligands are essential for mucosal protection and/or the adaptive response to external injury. Furthermore, disruption of ErbB signaling produces major defects in gut epithelial development and in the reparative response to gut injury,[25] illustrating the essential role of ErbB in gut mucosal growth.

Remarkably, the biology of GLP-2 in the gut overlaps to a considerable extent with actions of ErbB ligands and receptors. For example, the production of salivary EGF and the expression and activation of the EGFR are increased following major small bowel resection,[26] and both intestinal proglucagon gene expression and circulating levels of GLP-2 are increased following major small bowel resection.[27] Moreover both EGF and GLP-2 stimulate cell proliferation,[28,29] enhance mucosal adaptation

following small bowel resection,[30,31] and accelerate recovery of epithelial integrity following radiation-induced injury.[32,33] Similarly, both TGF-α and GLP-2 attenuate the severity of experimental colitis in mice.[34,35] Nevertheless, the extent to which GLP-2 exerts its actions in part via downstream recruitment of ErbB signaling effectors has not previously been identified.

Our data identify a new mechanism for the proliferative actions of GLP-2 via the rapid induction of a subset of ErbB ligands in both the small and large bowel (Figure 8*E*). Moreover, although the proliferative actions of GLP-2 in the gut have previously been linked to IGF-I[14,15] and KGF[11] in the small and large bowel, respectively, our findings illustrate that GLP-2, but not IGF-I or KGF, selectively activates ErbB ligands and their downstream immediate early gene targets in both small and large bowel. Moreover, the specificity of GLP-2 action on ErbB ligand expression was further illustrated by the demonstration that GLP-2 had no effect on expression of TGFs, IGFs, KGF, Vegfa, Tff3, and neurotensin (Supplementary Figure 5). These findings illustrate the complexity and selectivity of GLP-2 action and expand the identity of growth factor signaling networks activated by GLP-2 in the gastrointestinal tract.

Although GLP-2 mimics many EGF actions in the gut, EGF, but not GLP-2, robustly activated the expression of phosphorylated Akt in the outer longitudinal muscle layer of the colon, consistent with the trophic actions of EGF, but not GLP-2, on colonic smooth muscle.[36] Furthermore, GLP-2 increased nuclear c-fos expression in cells residing predominantly in the distal villus, whereas EGF produced robust c-fos expression within cells along the entire crypt to villus axis. Similarly, EGF produced a more widespread induction of c-fos expression in the colon, relative to the cellular pattern seen with GLP-2. Hence, the actions of GLP-2 overlap with, but are not identical to, those described for EGF in the murine gut.

Although the GLP-2-dependent induction of ErbB ligands and IEG expression was only modestly diminished in the *waved-2* mouse, the pan-ErbB inhibitor CI-1033 completely abrogated the GLP-2-mediated induction of ErbB ligand and IEG expression in the murine jejunum. Furthermore, CI-1033 selectively eliminated the proliferative response to GLP-2, but not KGF, in the jejunum. Hence, ErbB signaling is required for the GLP-2-mediated induction of a gene expression profile linked to stimulation of epithelial cell proliferation in the murine gut.

The observation that GLP-2 induces multiple ErbB ligands, principally, amphiregulin, epiregulin, and HB-EGF, suggests that these molecules may act in concert to activate ErbB signaling, leading to stimulation of crypt cell proliferation and expansion of the mucosal epithelium. Moreover, several peptide hormones, including GLP-1, directly transactivate the EGF receptor independent of the presence of ErbB ligands,[2] raising another possibility for linking GLP-2R signaling to ErbB receptor activation. A testable hypothesis involving ErbB receptors, IGF-1, and KGF as downstream mediators of GLP-2 action invokes the possibility that ErbB signaling may be upstream of and lead to IGF-1 and/or KGF activation. The known expression of ErbB1, ErbB2, ErbB3, amphiregulin, epiregulin, and HB-EGF in the intestinal mucosa, together with our current data linking GLP-2 action to induction of ErbB ligands and stimulation of cell proliferation, extends our understanding of GLP-2 action to encompass activation of the ErbB-signaling network. These findings may have implications for understanding the potential therapeutic efficacy and safety of GLP-2R agonists being developed for the treatment of human intestinal disorders.

Supplementary Data

Note: To access the supplementary material accompanying this article, visit the online version of *Gastroenterology* at www.gastrojournal.org, and at doi: 10.1053/j.gastro.2009.05.057.

References

1. Drucker DJ. The biology of incretin hormones. Cell Metab 2006; 3:153–165.
2. Buteau J, Foisy S, Joly E, et al. Glucagon-like peptide 1 induces pancreatic β-cell proliferation via transactivation of the epidermal growth factor receptor. Diabetes 2003;52:124–132.
3. Munroe DG, Gupta AK, Kooshesh F, et al. Prototypic G protein-coupled receptor for the intestinotrophic factor glucagon-like peptide 2. Proc Natl Acad Sci U S A 1999;96:1569–1573.
4. Mayo KE, Miller LJ, Bataille D, et al. International Union of Pharmacology. XXXV. The glucagon receptor family. Pharmacol Rev 2003;55:167–194.
5. Yusta B, Estall J, Drucker DJ. GLP-2 receptor activation engages Bad and glycogen synthase kinase 3 in a protein kinase A-dependent manner and prevents apoptosis following inhibition of phosphatidylinositol 3-kinase. J Biol Chem 2002;277:24896–24906.
6. Burrin DG, Stoll B, Guan X, et al. Glucagon-like peptide 2 dose-dependently activates intestinal cell survival and proliferation in neonatal piglets. Endocrinology 2005;146:22–32.
7. Bjerknes M, Cheng H. Modulation of specific intestinal epithelial progenitors by enteric neurons. Proc Natl Acad Sci U S A 2001; 98:12497–12502.
8. Guan X, Karpen HE, Stephens J, et al. GLP-2 receptor localizes to enteric neurons and endocrine cells expressing vasoactive peptides and mediates increased blood flow. Gastroenterology 2006;130:150–164.
9. Nelson DW, Sharp JW, Brownfield MS, et al. Localization and activation of glucagon-like peptide-2 receptors on vagal afferents in the rat. Endocrinology 2007;148:1954–1962.
10. Yusta B, Huang L, Munroe D, et al. Enteroendocrine localization of GLP-2 receptor expression. Gastroenterology 2000;119:744–755.
11. Orskov C, Hartmann B, Poulsen SS, et al. GLP-2 stimulates colonic growth via KGF, released by subepithelial myofibroblasts with GLP-2 receptors. Regul Pept 2005;124:105–112.
12. Sigalet DL, Wallace LE, Holst JJ, et al. Enteric neural pathways mediate the anti-inflammatory actions of glucagon-like peptide 2. Am J Physiol Gastrointest Liver Physiol 2007;293:G211–G221.
13. Guan X, Stoll B, Lu X, et al. GLP-2-mediated up-regulation of intestinal blood flow and glucose uptake is nitric oxide-dependent in TPN-fed piglets 1. Gastroenterology 2003;125:136–147.

14. Dube PE, Forse CL, Bahrami J, et al. The essential role of insulin-like growth factor-1 in the intestinal tropic effects of glucagon-like peptide-2 in mice. Gastroenterology 2006;131:589–605.
15. Dube PE, Rowland KJ, Brubaker PL. Glucagon-like peptide-2 activates β-catenin signaling in the mouse intestinal crypt: role of insulin-like growth factor-I. Endocrinology 2008;149:291–301.
16. Walters JR. Cell and molecular biology of the small intestine: new insights into differentiation, growth and repair. Curr Opin Gastroenterol 2004;20:70–76.
17. Koehler JA, Harper W, Barnard M, et al. Glucagon-like peptide-2 does not modify the growth or survival of murine or human intestinal tumor cells. Cancer Res 2008;68:7897–7904.
18. Luetteke NC, Phillips HK, Qiu TH, et al. The mouse waved-2 phenotype results from a point mutation in the EGF receptor tyrosine kinase. Genes Dev 1994;8:399–413.
19. Christensen JG, Vincent PW, Klohs WD, et al. Plasma vascular endothelial growth factor and interleukin-8 as biomarkers of antitumor efficacy of a prototypical erbB family tyrosine kinase inhibitor. Mol Cancer Ther 2005;4:938–947.
20. Nyati MK, Maheshwari D, Hanasoge S, et al. Radiosensitization by pan ErbB inhibitor CI-1033 in vitro and in vivo. Clin Cancer Res 2004;10:691–700.
21. Koehler JA, Yusta B, Drucker DJ. The HeLa cell glucagon-like peptide-2 receptor is coupled to regulation of apoptosis and ERK1/2 activation through divergent signaling pathways. Mol Endocrinol 2005;19:459–473.
22. Nowak M, Gaines GC, Rosenberg J, et al. LPS-induced liver injury in D-galactosamine-sensitized mice requires secreted TNF-α and the TNF-p55 receptor. Am J Physiol Regul Integr Comp Physiol 2000;278:R1202–R1209.
23. Solorzano CC, Ksontini R, Pruitt JH, et al. Involvement of 26-kDa cell-associated TNF-α in experimental hepatitis and exacerbation of liver injury with a matrix metalloproteinase inhibitor. J Immunol 1997;158:414–419.
24. Citri A, Yarden Y. EGF-ERBB signalling: towards the systems level. Nat Rev Mol Cell Biol 2006;7:505–516.
25. Helmrath MA, Erwin CR, Warner BW. A defective EGF-receptor in waved-2 mice attenuates intestinal adaptation. J Surg Res 1997; 69:76–80.
26. Warner BW, Erwin CR. Critical roles for EGF receptor signaling during resection-induced intestinal adaptation. J Pediatr Gastroenterol Nutr 2006;43(Suppl 1):S68–S73.
27. Dahly EM, Gillingham MB, Guo Z, et al. Role of luminal nutrients and endogenous GLP-2 in intestinal adaptation to mid-small bowel resection. Am J Physiol Gastrointest Liver Physiol 2003; 284:G670–G682.
28. Al-Nafussi AI, Wright NA. The effect of epidermal growth factor (EGF) on cell proliferation of the gastrointestinal mucosa in rodents. Virchows Arch 1982;40:63–69.
29. Drucker DJ, Ehrlich P, Asa SL, et al. Induction of intestinal epithelial proliferation by glucagon-like peptide 2. Proc Natl Acad Sci U S A 1996;93:7911–7916.
30. Chaet MS, Arya G, Ziegler MM, et al. Epidermal growth factor enhances intestinal adaptation after massive small bowel resection. J Pediatr Surg 1994;29:1035–1039.
31. Scott RB, Kirk D, MacNaughton WK, et al. GLP-2 augments the adaptive response to massive intestinal resection in rat. Am J Physiol 1998;275:G911–G921.
32. Lee KK, Jo HJ, Hong JP, et al. Recombinant human epidermal growth factor accelerates recovery of mouse small intestinal mucosa after radiation damage. Int J Radiat Oncol Biol Phys 2008;71:1230–1235.
33. Torres S, Thim L, Milliat F, et al. Glucagon-like peptide-2 improves both acute and late experimental radiation enteritis in the rat. Int J Radiat Oncol Biol Phys 2007;69:1563–1571.
34. Drucker DJ, Yusta B, Boushey RP, et al. Human [Gly2]-GLP-2 reduces the severity of colonic injury in a murine model of experimental colitis. Am J Physiol 1999;276:G79–G91.
35. Egger B, Carey HV, Procaccino F, et al. Reduced susceptibility of mice overexpressing transforming growth factor α to dextran sodium sulphate colitis. Gut 1998;43:64–70.
36. Ribbons KA, Howarth GS, Davey KB, et al. Subcutaneous but not intraluminal epidermal growth factor stimulates colonic growth in normal adult rats. Growth Factors 1994;10:153–162.

Received October 1, 2008. Accepted May 29, 2009.

Reprint requests

Address requests for reprints to: Daniel J. Drucker, MD, Mt. Sinai Hospital SLRI, 60 Murray Street, Mailbox 39, Toronto, Ontario, Canada M5T 3L9. e-mail: d.drucker@utoronto.ca; fax: (416) 361-2669.

Acknowledgments

The authors thank Dr Robin Boushey and Seung–Jun Lee for assistance with some experiments.

Conflicts of interest

The authors disclose the following: Dr Drucker is a party, together with the University of Toronto and the University Health Network, in a GLP-2 licensing agreement with NPS Pharmaceuticals Inc. The remaining authors disclose no conflicts.

Funding

Supported in part by an operating grant from CIHR MOP-14799 and from the National Cancer Institute of Canada, grant 017428; by the Canadian Cancer Society; and by a Canada Research Chair in Regulatory Peptides (to D.J.D.).

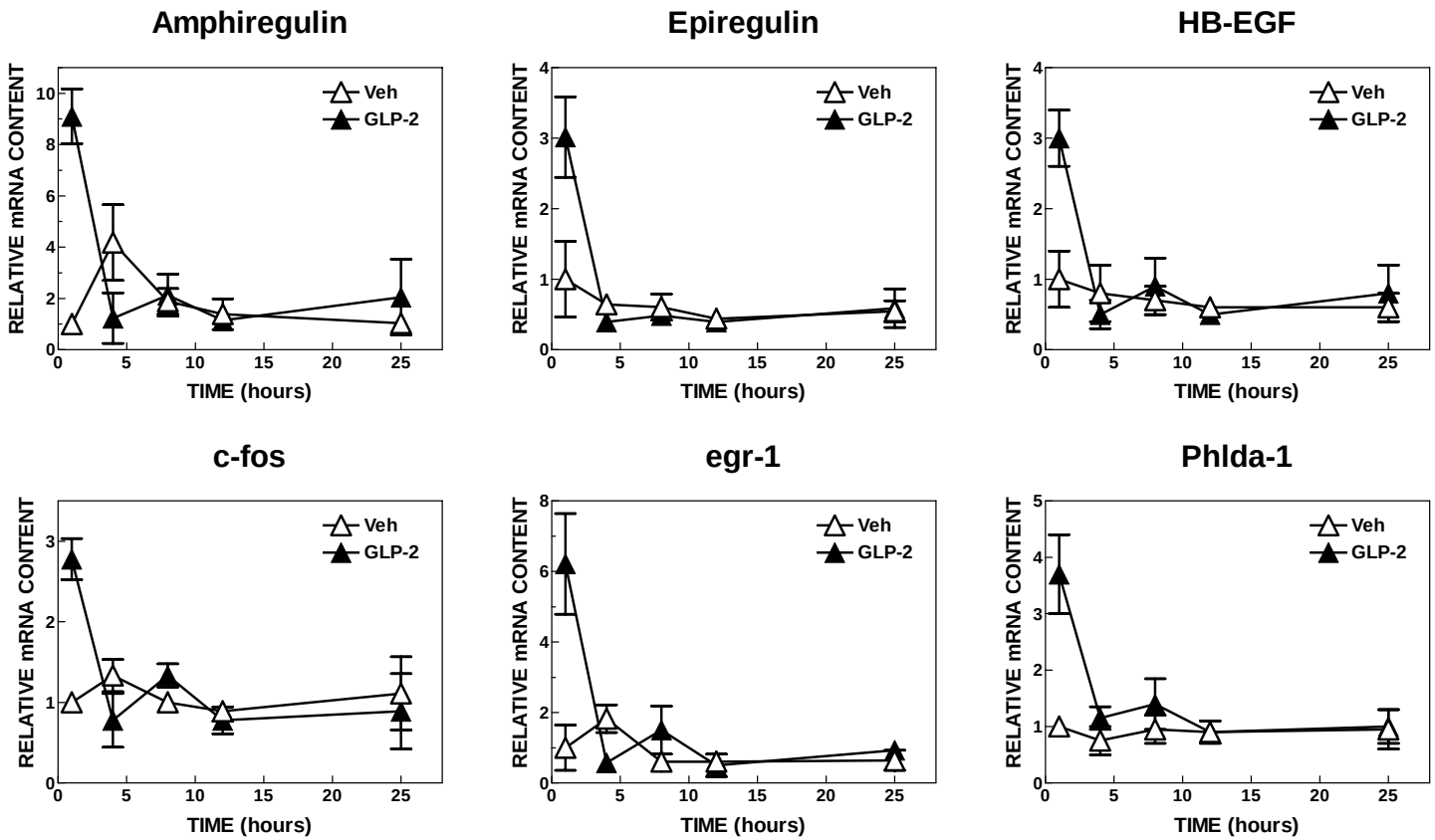
Amphiregulin
Epiregulin
HB-EGF
c-fos
egr-1
Phlda-1
RELATIVE mRNA CONTENT
TIME (hours)
Veh
GLP-2

Supp Fig 1

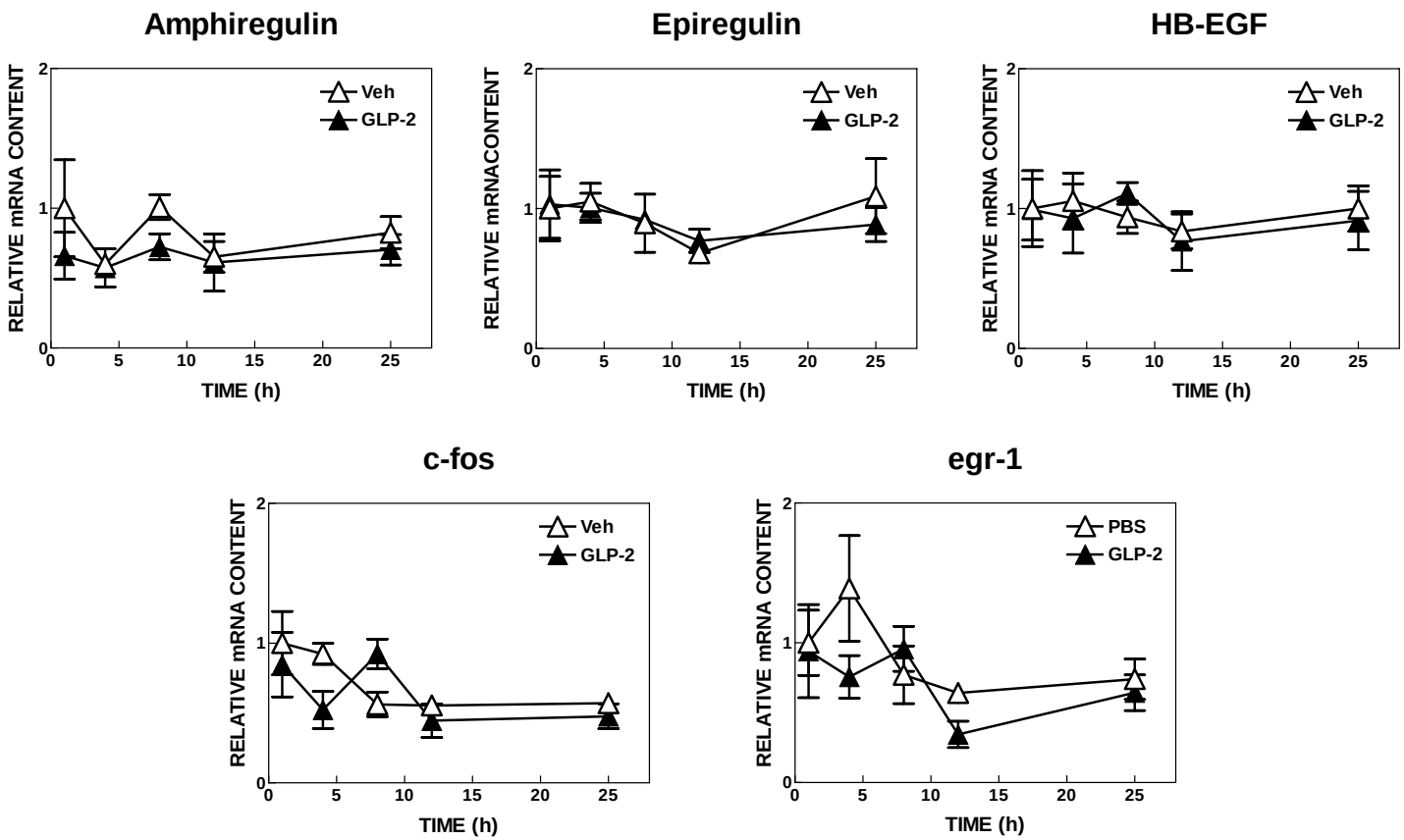
Amphiregulin
Epiregulin
HB-EGF
c-fos
egr-1
RELATIVE mRNA CONTENT
TIME (h)
Veh
GLP-2
PBS
0
1
2
0
5
10
15
20
25

Supp Fig 2

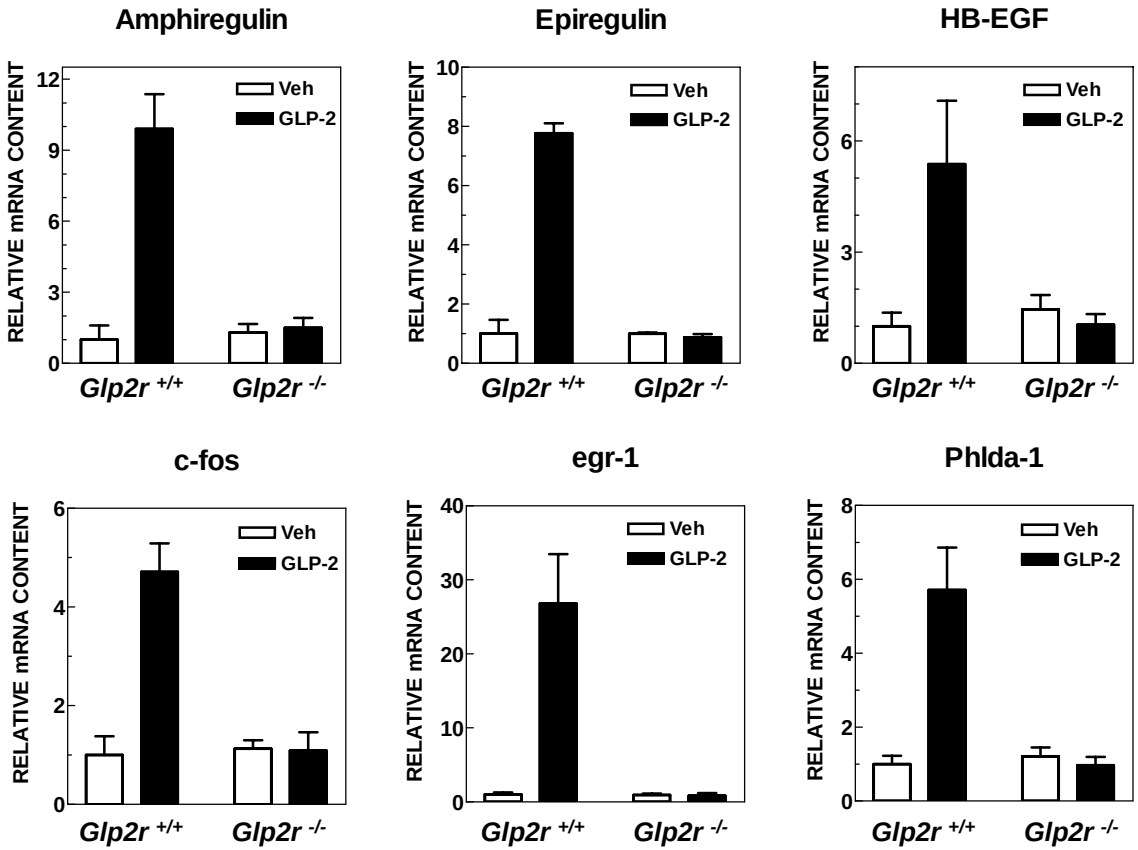
Amphiregulin
Epiregulin
HB-EGF
c-fos
egr-1
Phlda-1
RELATIVE mRNA CONTENT
Veh
GLP-2
Glp2r +/+
Glp2r -/-

Supp Fig 3

A

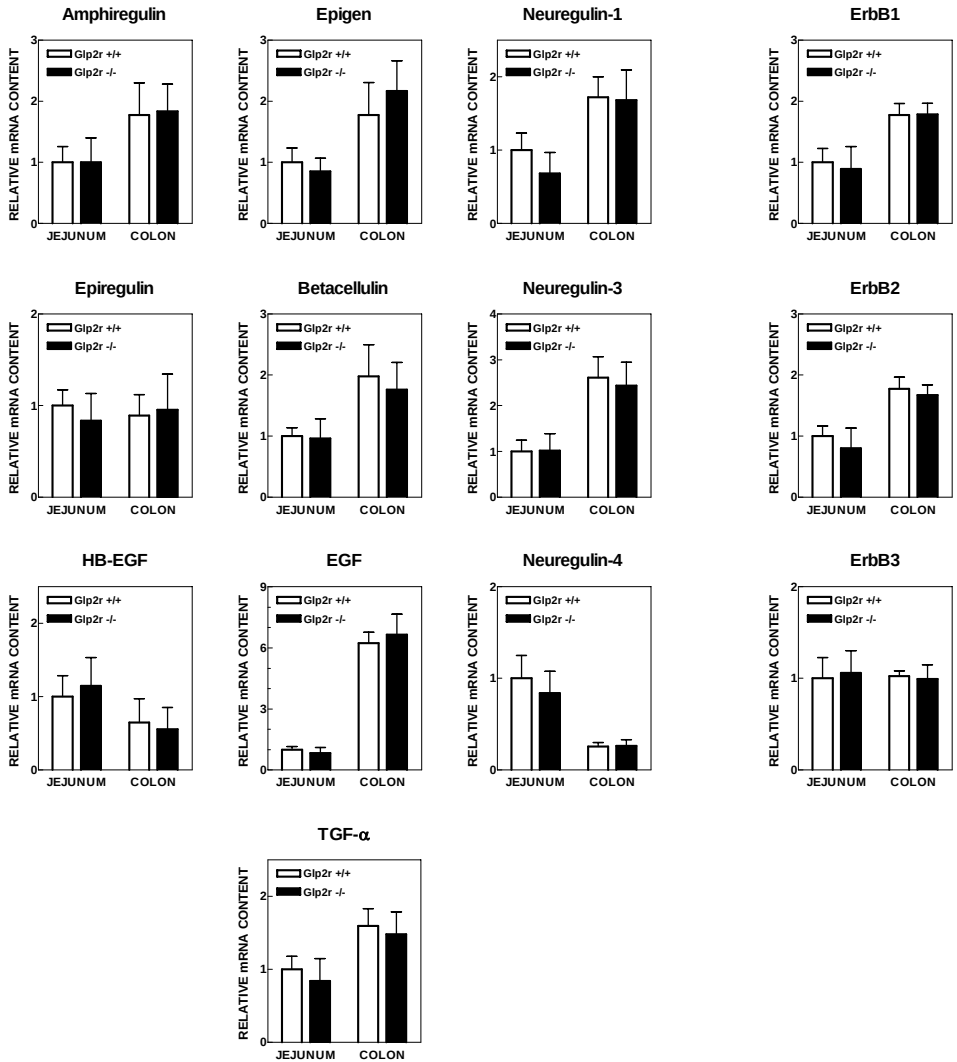
Amphiregulin
Epigen
Neuregulin-1
ErbB1
Epiregulin
Betacellulin
Neuregulin-3
ErbB2
HB-EGF
EGF
Neuregulin-4
ErbB3
TGF-α
Glp2r +/+
Glp2r -/-
RELATIVE mRNA CONTENT
JEJUNUM
COLON

Supp Fig 4A

B

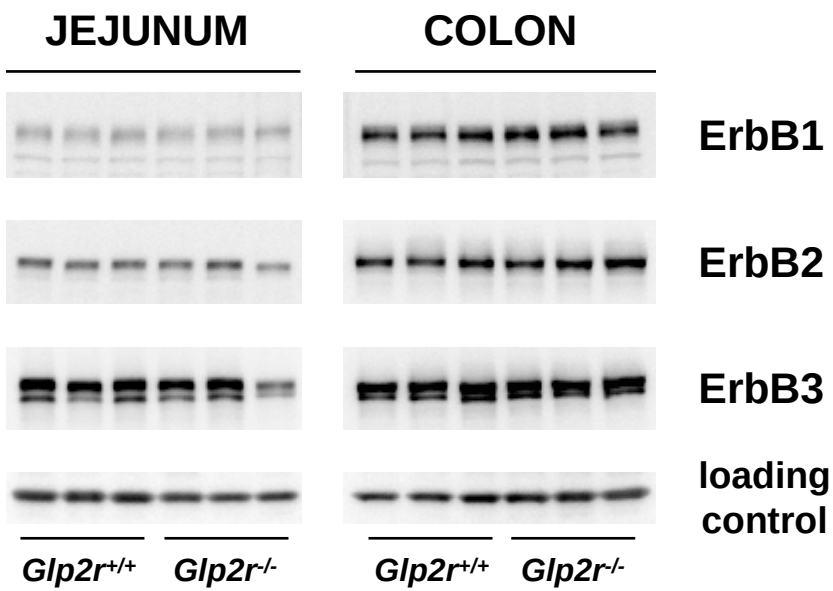
JEJUNUM
COLON
ErbB1
ErbB2
ErbB3
loading control
Glp2r+/+
Glp2r-/-
Glp2r+/+
Glp2r-/-

Supp Fig 4B

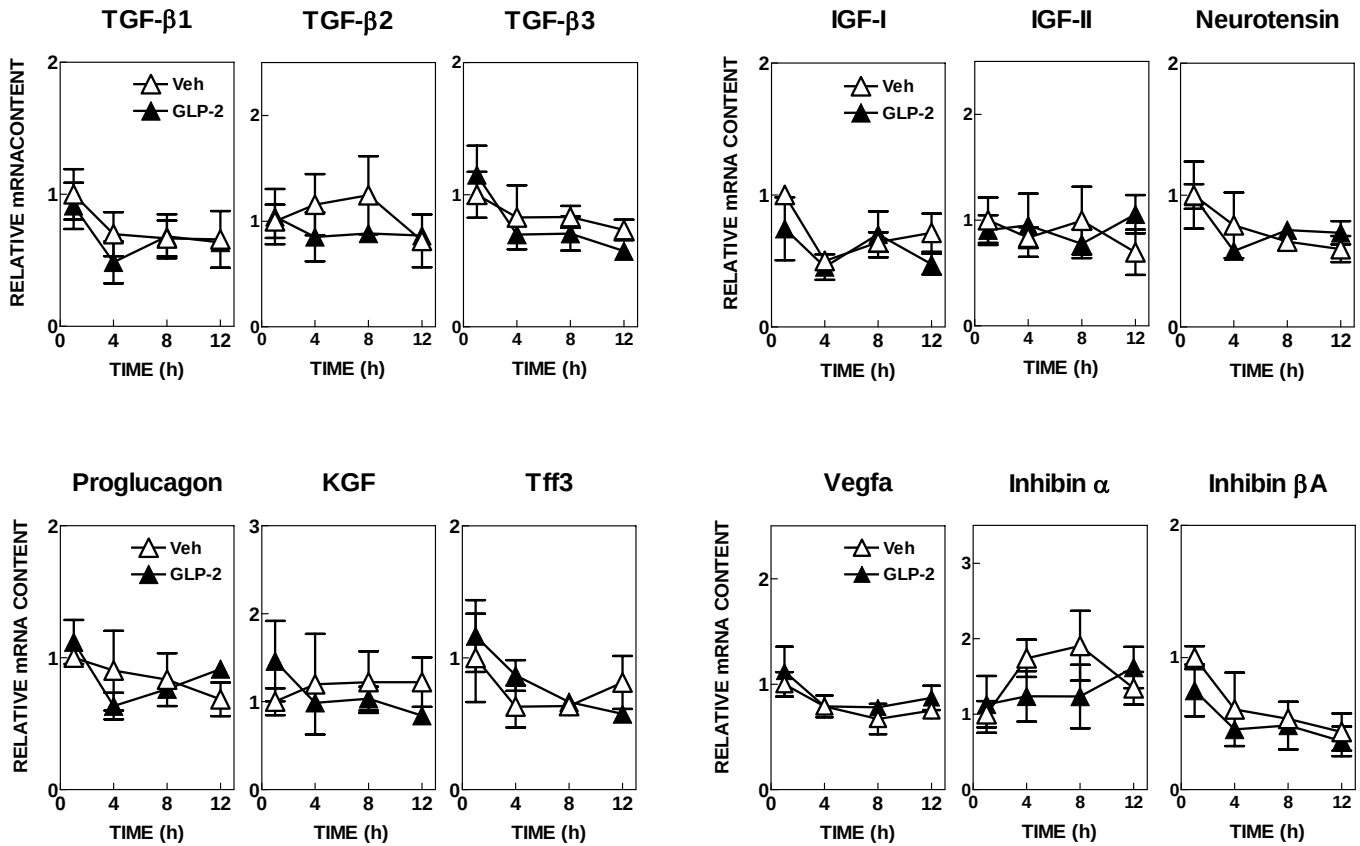
TGF-β1
TGF-β2
TGF-β3
IGF-I
IGF-II
Neurotensin
Proglucagon
KGF
Tff3
Vegfa
Inhibin α
Inhibin βA
Veh
GLP-2
RELATIVE mRNACONTENT
RELATIVE mRNA CONTENT
TIME (h)

Supp Fig 5

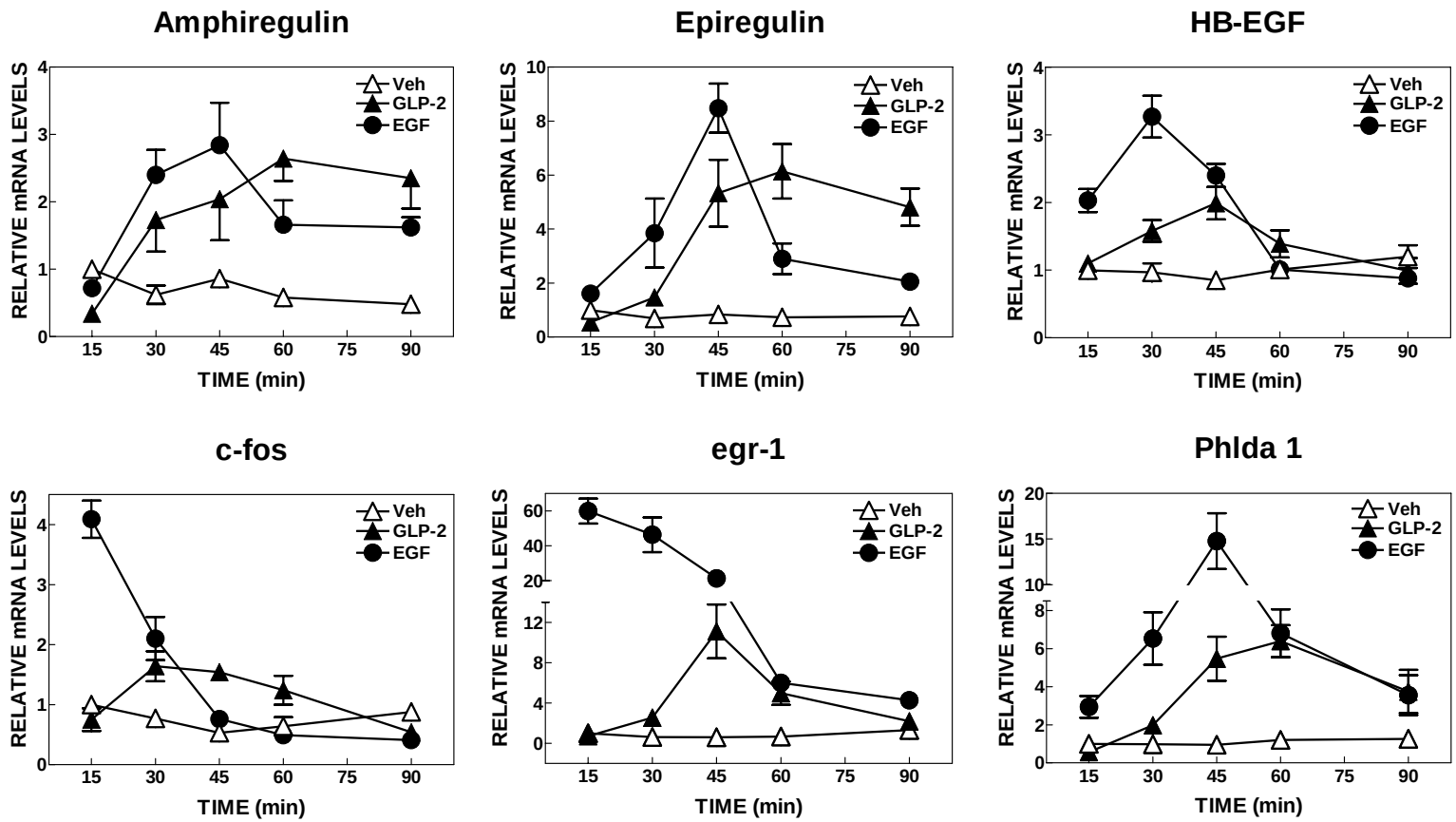
Amphiregulin
Epiregulin
HB-EGF
c-fos
egr-1
Phlda 1
RELATIVE mRNA LEVELS
TIME (min)
Veh
GLP-2
EGF
15
30
45
60
75
90

Supp Fig 6

A

P-(Ser473) Akt staining

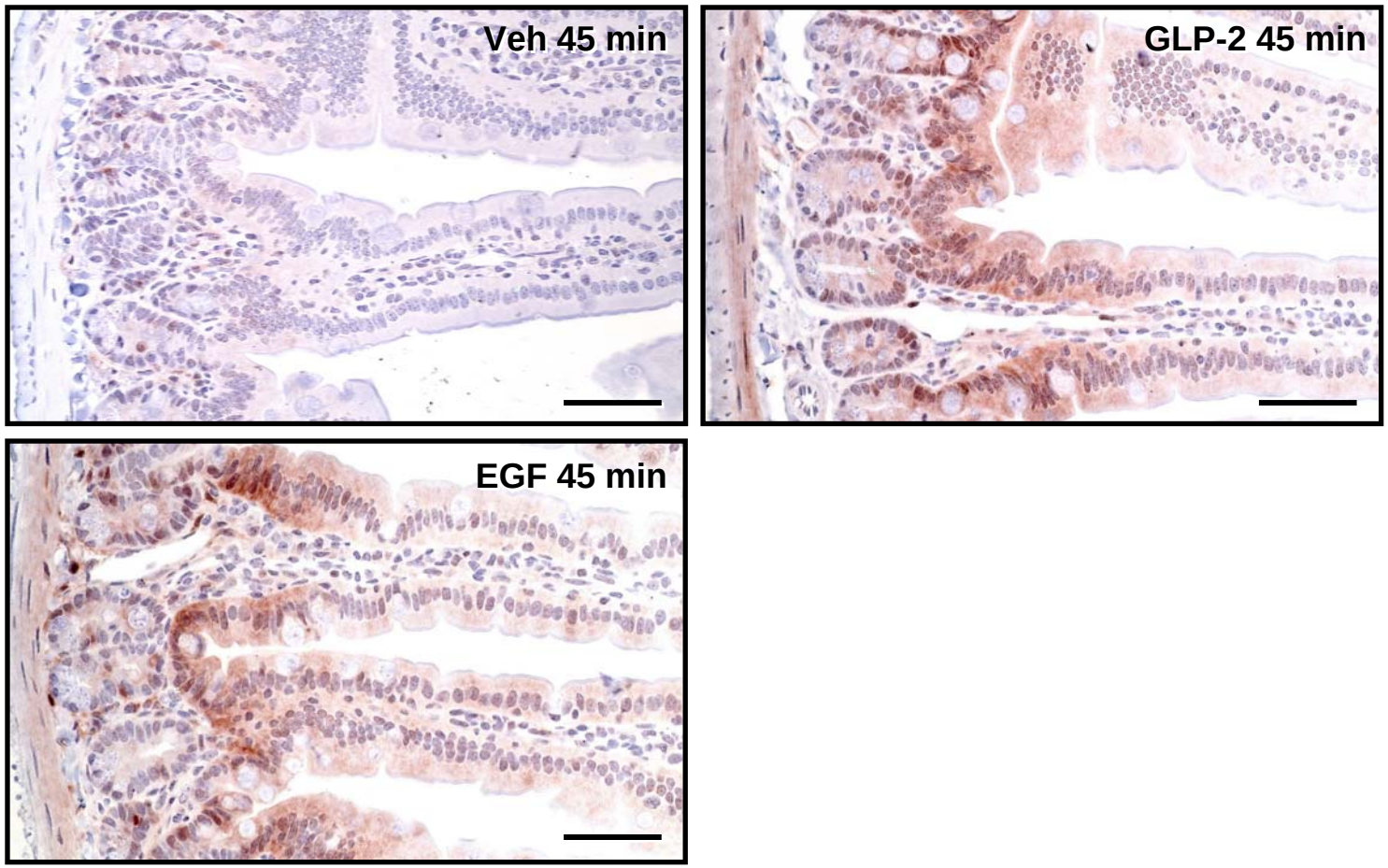

Supp Fig 7A

B

P-(Ser473) Akt staining

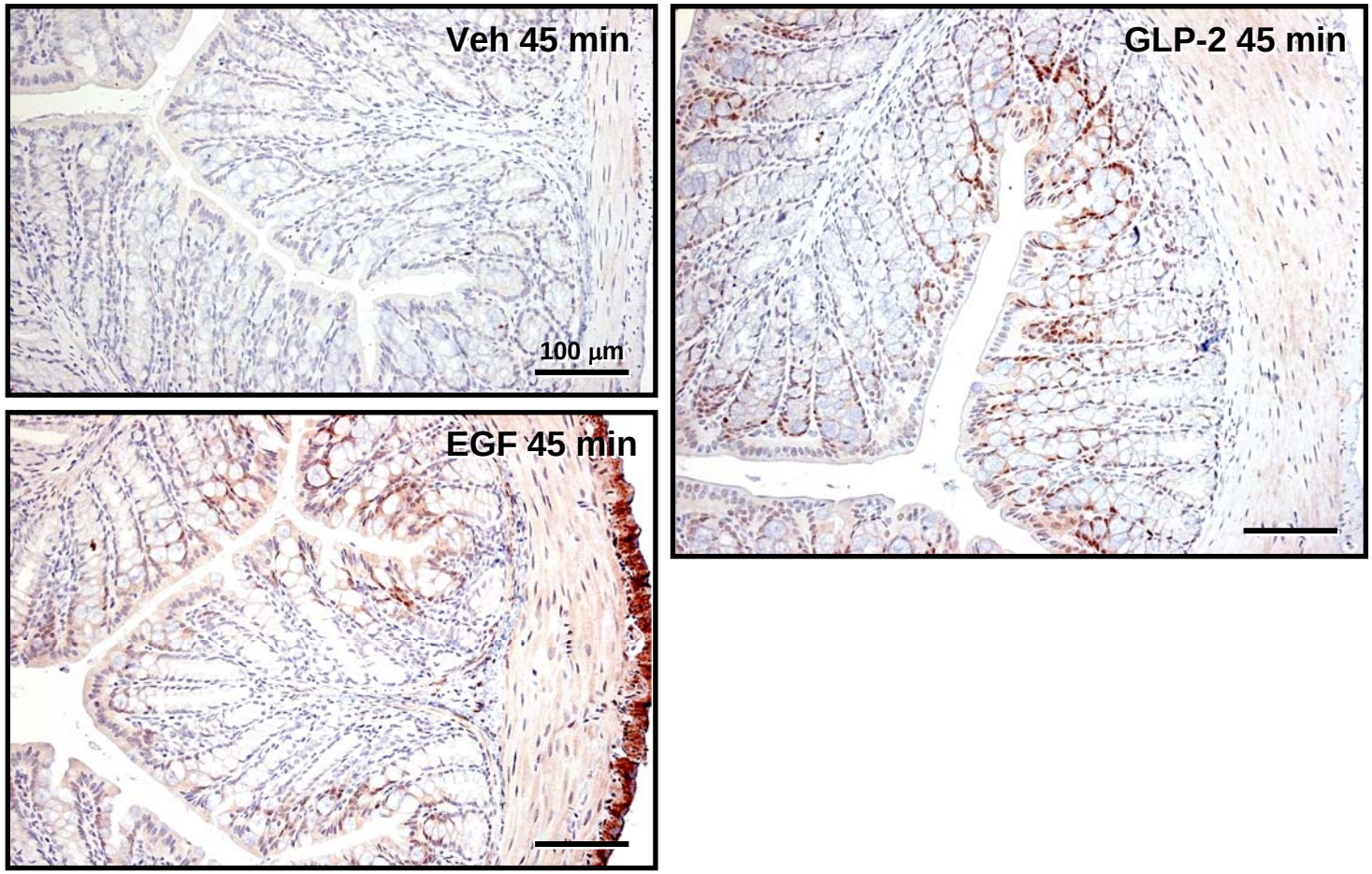

Supp Fig 7B

c-fos staining

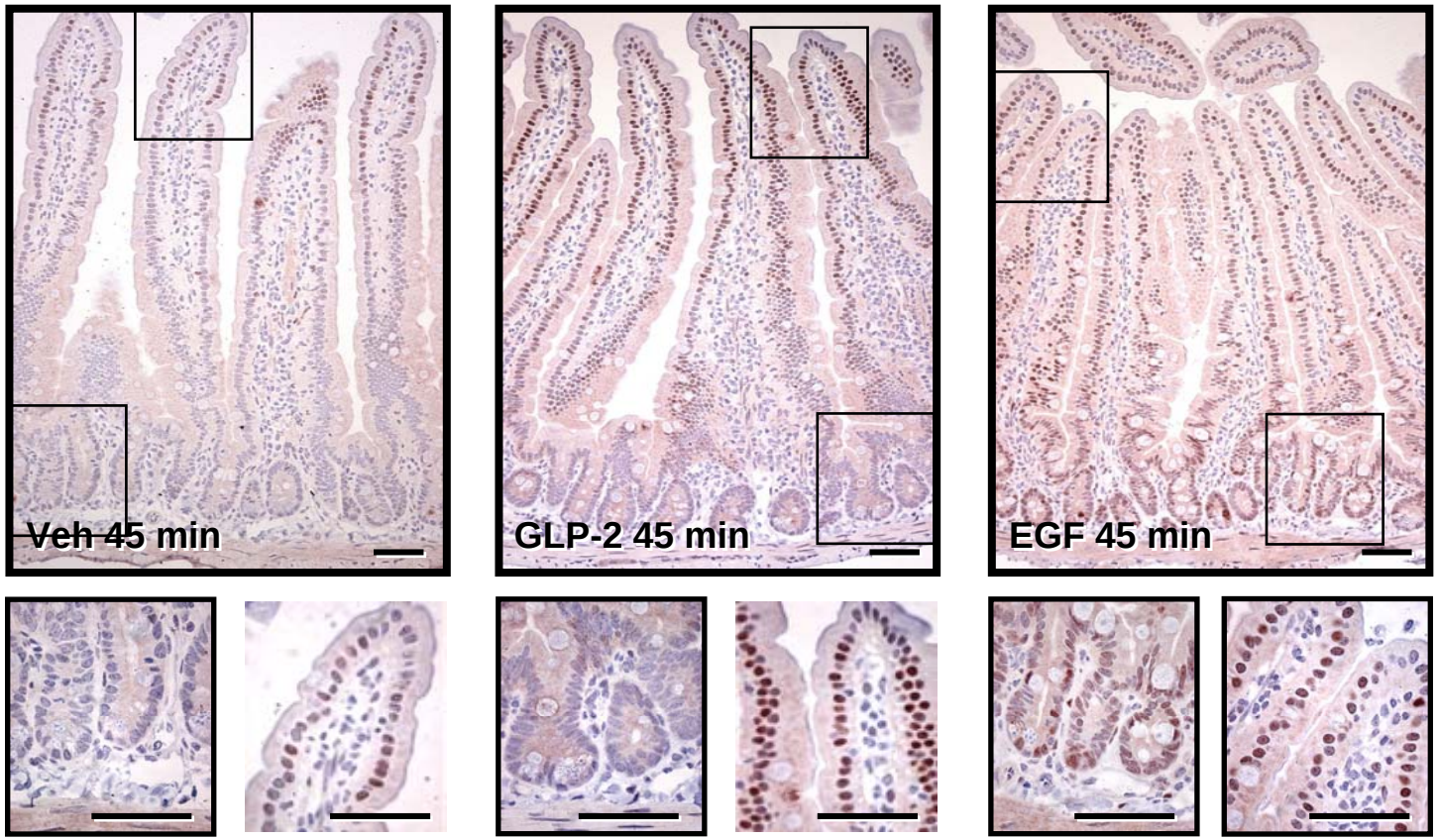

Supp Fig 8

c-fos staining

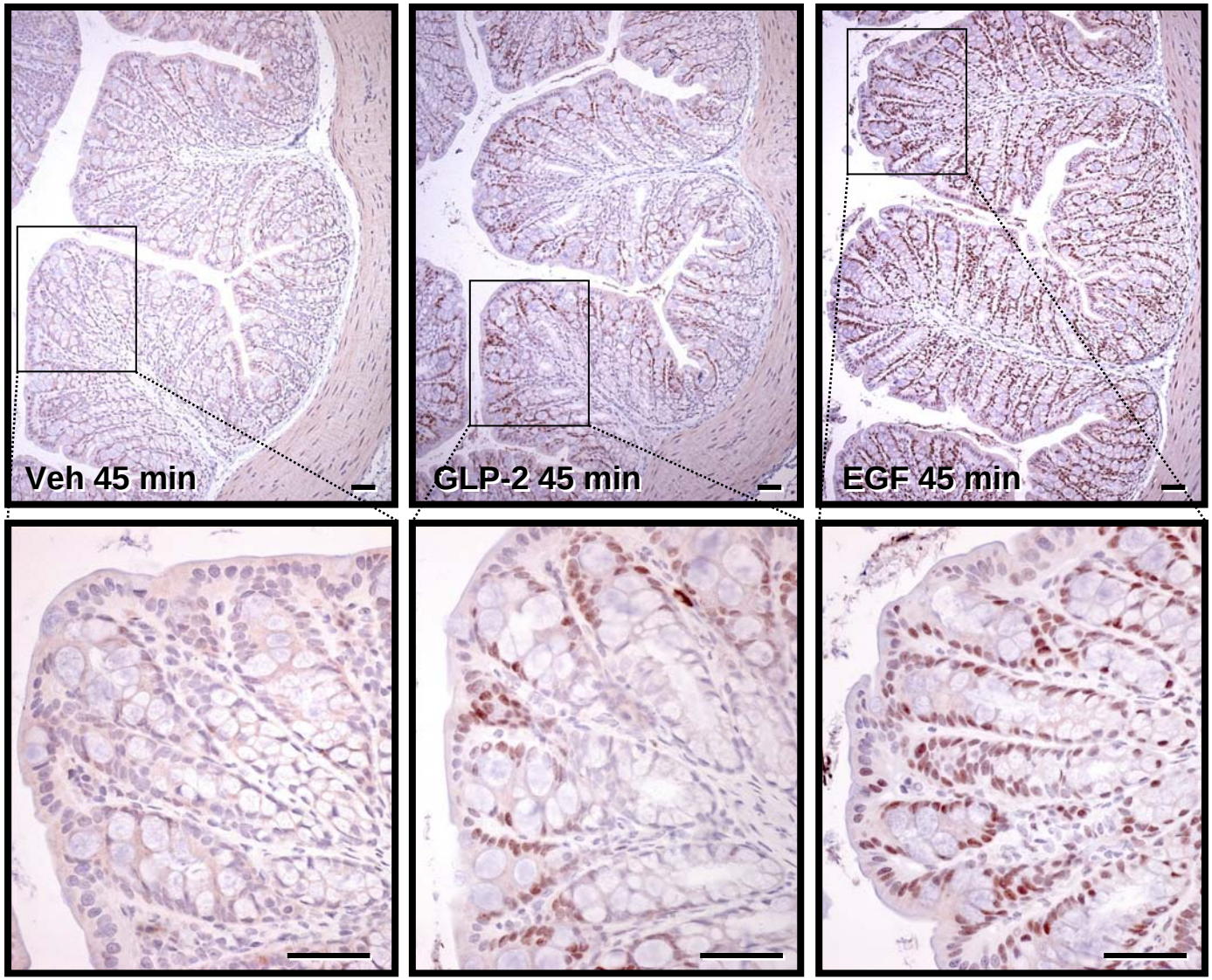

Supp Fig 9

A

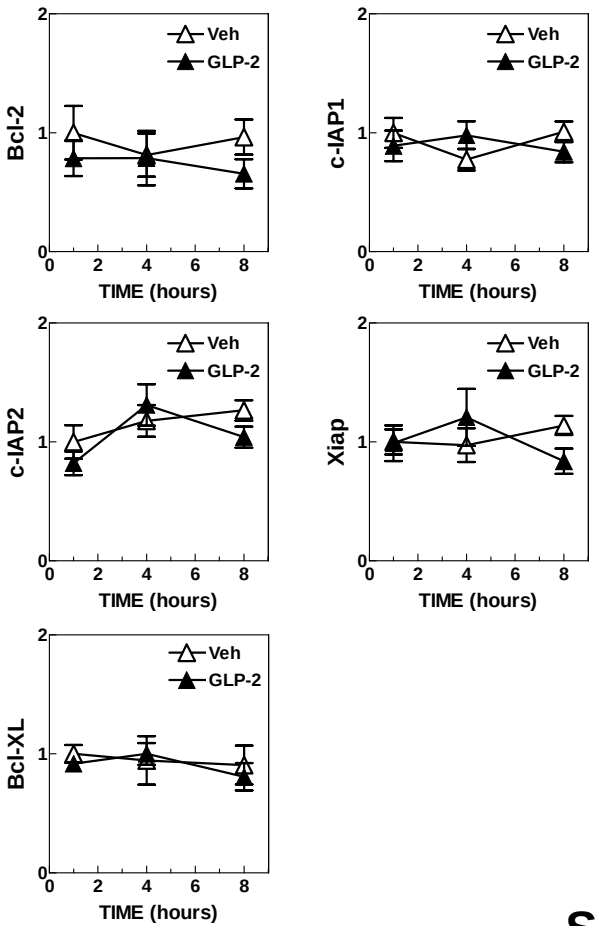

B

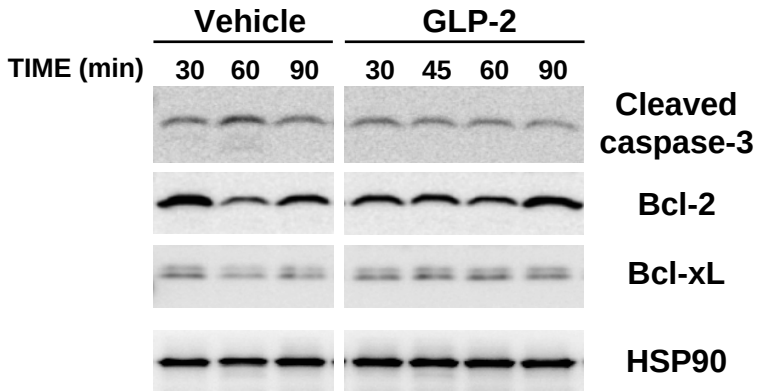

Supp Fig 10

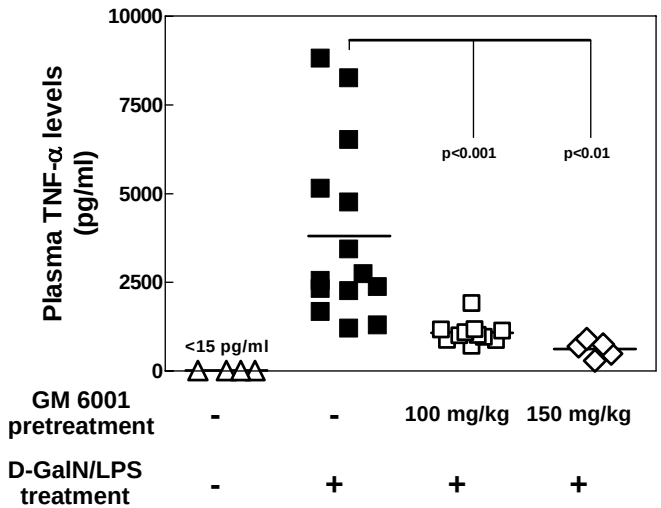
Plasma TNF-α levels (pg/ml)
10000
7500
5000
2500
0
p<0.001
p<0.01
<15 pg/ml
GM 6001 pretreatment
- - 100 mg/kg 150 mg/kg
D-GalN/LPS treatment
- + + +

Supp Fig 11

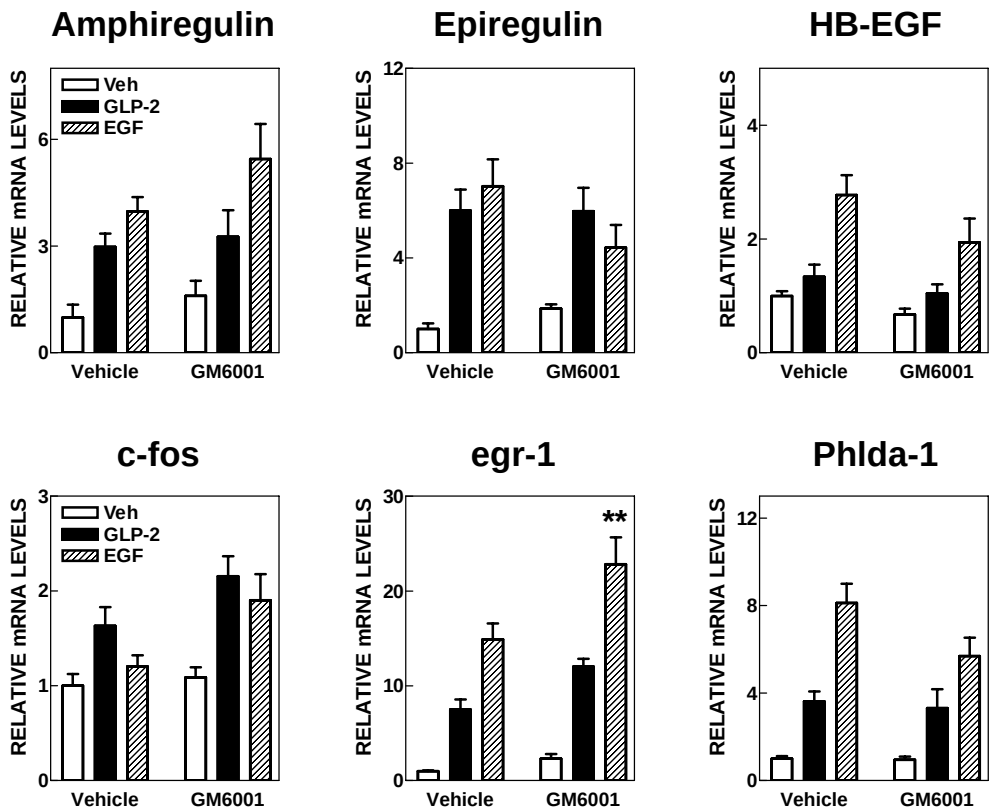
Amphiregulin
Epiregulin
HB-EGF
c-fos
egr-1
Phlda-1
RELATIVE mRNA LEVELS
Veh
GLP-2
EGF
Vehicle
GM6001
**

Supp Fig 12

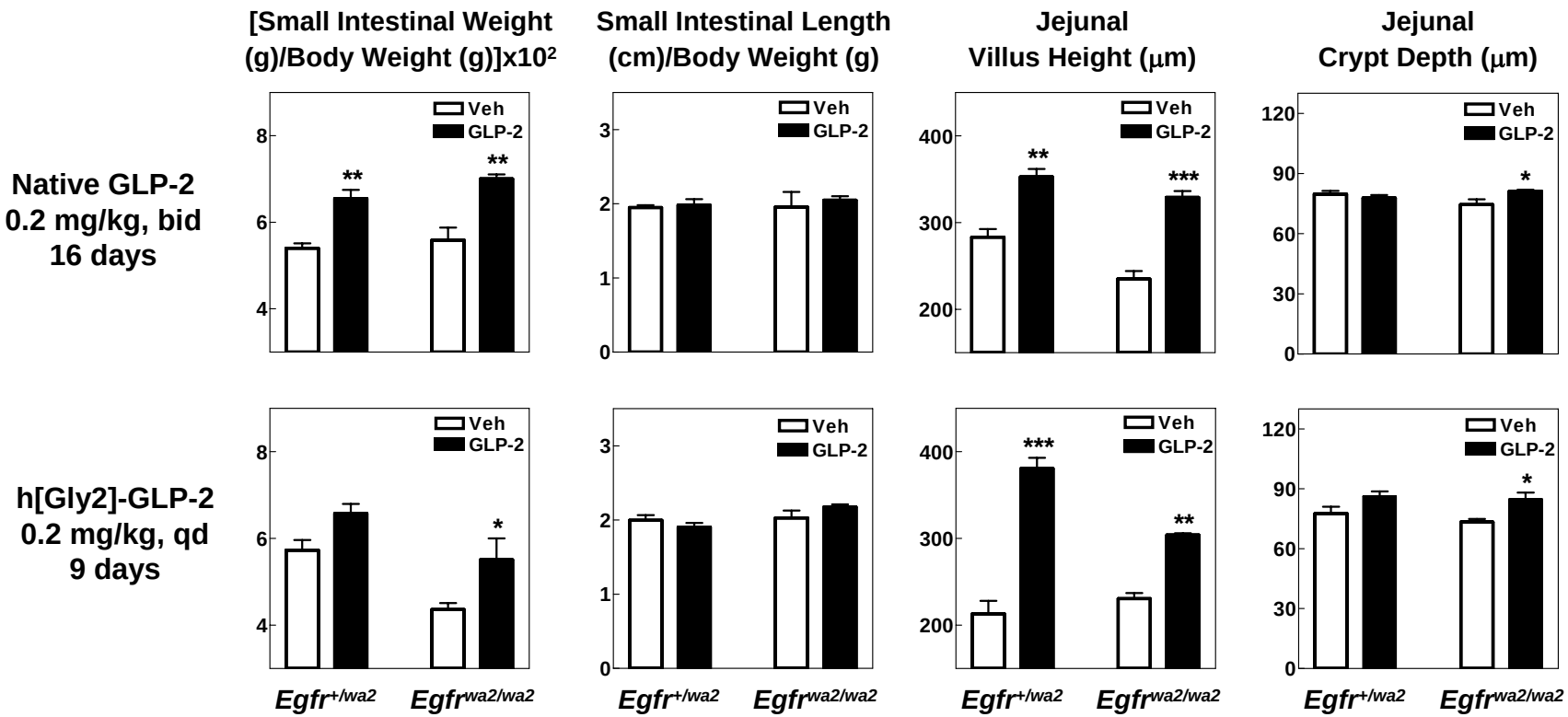
[Small Intestinal Weight (g)/Body Weight (g)]x10²
Small Intestinal Length (cm)/Body Weight (g)
Jejunal Villus Height (μm)
Jejunal Crypt Depth (μm)
Native GLP-2
0.2 mg/kg, bid
16 days
h[Gly2]-GLP-2
0.2 mg/kg, qd
9 days
Veh
GLP-2
Egfr+/wa2
Egfrwa2/wa2

Supp Fig 13

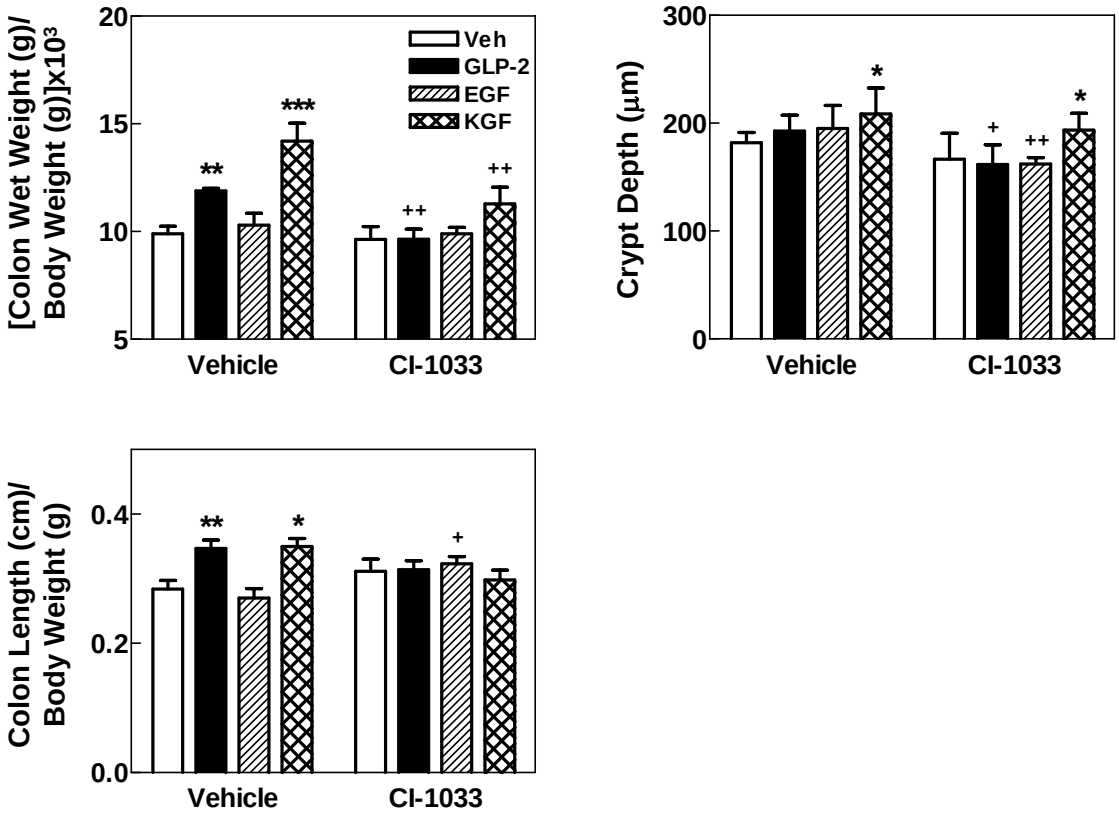
[Colon Wet Weight (g)/
Body Weight (g)]x10³
20
15
10
5
Veh
GLP-2
EGF
KGF
**
***
++
++
Vehicle
CI-1033
Crypt Depth (μm)
300
200
100
0
*
+
++
*
Vehicle
CI-1033
Colon Length (cm)/
Body Weight (g)
0.4
0.2
0.0
**
*
+
Vehicle
CI-1033

Supp Fig 14

Supplementary Fig Legends

Supp Fig 1. Acute induction of ErbB ligand and IEG transcripts by GLP-2 in mouse colon. Levels of the indicated transcripts were determined by real-time quantitative RT-PCR analysis of total RNA isolated from colon of CD1 mice sacrificed 1, 4, 8, 12 and 25 hours following a single injection of GLP-2 (0.2 mg/kg) or vehicle alone (PBS). Data, presented as fold-induction relative to the vehicle treatment group at time 1 hour, are means ± SE of two independent experiments involving a total of 3 mice per condition. SE for data with coefficients of variation ≤5% is not visible on the graph.

Supp Fig 2. GLP-2 does not regulate the expression of ErbB ligand, c-fos and egr-1 transcripts in mouse stomach. CD1 mice were sacrificed at 1, 4, 8, 12 and 25 hours following a single injection of GLP-2 (0.2 mg/kg) or vehicle alone (PBS). Total RNA was isolated from stomach samples and reverse transcribed into cDNA. Levels of the indicated transcripts were determined by real-time quantitative PCR and are presented as fold-induction relative to the vehicle treatment group at time 1 hour. Data are means ± SE of two independent experiments involving a total of 3 mice per condition. SE for data with coefficients of variation ≤5% is not visible on the graph.

Supp Fig 3. The GLP-2 receptor is essential for GLP-2-dependent induction of ErbB ligand and IEG transcripts in mouse jejunum. Total RNA was isolated from jejunum of 10 weeks old littermate male mice of the indicated *Glp2r* genotype treated with h[Gly2]GLP-2 (0.2 mg/kg) or vehicle alone (PBS) for 60 min. mRNA levels of the specified ErbB ligands and IEGs were determined by real-time quantitative RT-PCR analysis and are presented as fold-induction relative to the vehicle-treated $Glp2r^{+/+}$ mice. Data are means ± SE of two independent experiments involving a total of 3-4 mice per genotype and condition. Consistent with observations in jejunum, GLP-2 did not upregulate ErbB ligand and IEG transcripts in the colon of $Glp2r^{-/-}$ mice.

Supp Fig 4. The lack of GLP-2 receptor signaling does not affect the expression of ErbB ligand and receptors in the mouse intestine. Intestinal tissue samples from 8-10 weeks old littermate male mice of the specified *Glp2r* genotype were collected for RNA and Western blot analyses. *(A)* mRNA levels of the indicated transcripts were determined by real-time quantitative RT-PCR and expressed relative to the jejunal $Glp2r^{+/+}$ values. Data are means ± SE of two independent

experiments involving a total of 7 mice per genotype. *(B)* Whole tissue extracts from 3 of each *Glp2r*$^{+/+}$ and *Glp2r*$^{-/-}$ mice analyzed by immunoblotting for ErbB1, ErbB2 and ErbB3. An unidentified ≅60 kDa protein crossreacting with the anti-ErbB2 antibody is shown to document loading and transfer conditions. Consistent with the very low levels of ErbB4 mRNA in mouse intestine (Ct values ≥32-34 by quantitative RT-PCR analysis), the ErbB4 protein was undetectable following immunoprecipitation of gut lysates with an anti-ErbB4 antibody and Western blotting with the same antibody, which readily immunoprecipitated ErbB4 from murine whole brain lysates (data not shown).

Supp Fig 5. GLP-2 does not regulate the expression of numerous intestinal growth/mucosal integrity factors in mouse jejunum. Total RNA was isolated from jejunum and colon of CD1 mice treated with GLP-2 (0.2 mg/kg) or vehicle alone (PBS) for the specified periods of time. Levels of the indicated transcripts were determined by real-time quantitative RT-PCR and expressed relative to the vehicle values at time 1 hour. Data are means ± SE of two independent experiments (3 mice per condition). No effect of GLP-2 was observed either when the mRNA levels of the same group of genes were assessed in mouse colon.

Supp Fig 6. Coordinated induction of specific ErbB ligand and IEG transcripts by GLP-2 and EGF in mouse jejunum. CD1 mice were euthanized at the indicated times following treatment with GLP-2 (0.2 mg/kg), EGF (1 mg/kg) or vehicle alone (PBS). Total RNA was isolated from jejunum tissue samples and reverse transcribed into cDNA. Levels of ErbB ligand and IEG transcripts were determined by real-time quantitative PCR and presented as fold-induction relative to the values of the vehicle group at time 15 min. Data are means ± SE of two independent experiments involving a total of 4 mice per condition. SE for data with coefficients of variation ≤5% is not visible on the graph.

Supp Fig 7. GLP-2 and EGF induce Akt activation in the murine intestinal mucosal epithelium. Immunohistochemical localization of active phospho-Ser473-Akt in transverse cross sections from jejunum (*A*) and colon (*B*) of mice treated for 45 min with GLP-2 (0.2 mg/kg), EGF (1 mg/kg) or vehicle alone (PBS). Photomicrographs are representative of 3-4 mice per group. Scale bars, 50 and 100 μm for *A* and *B*, respectively.

Supp Fig 8. GLP-2 and EGF induce nuclear c-fos expression in the murine jejunal mucosal epithelium. CD1 mice were sacrificed 45 min following s.c. injection of GLP-2 (0.2 mg/kg), EGF (1 mg/kg) or vehicle alone (PBS) and jejunal tissue samples were collected for

immunohistochemical localization of c-fos. The bottom panels are close-ups of the crypt and villus tips boxed in the upper panels. Photomicrographs are representative of 3-4 mice per group. Scale bars, 50 μm. GLP-2-induced c-fos positive nuclei accumulated in the epithelial cells lining the top half of the villi, whereas EGF-induced c-fos positive nuclei were found distributed in the epithelium along the entire crypt-villus axis.

Supp Fig 9. GLP-2 and EGF induce nuclear c-fos expression in the murine colonic mucosal epithelium. Immunohistochemical detection of c-fos in colon tissue sections of CD1 mice treated for 45 min with GLP-2 (0.2 mg/kg), EGF (1 mg/kg) or vehicle alone (PBS). The areas selected within the inset boxes are shown at a higher magnification. Photomicrographs are representative of 3-4 mice per group. Scale bars, 50 μm.

Supp Fig 10. GLP-2 does not acutely regulates caspase-3 cleavage or the expression of multiple apoptosis modulators in mouse jejunum. Jejunal tissue samples from CD1 mice treated for the specified periods of time with GLP-2 (0.2 mg/kg) or vehicle alone (PBS) were collected for RNA and Western blot analyses. *(A)* mRNA levels of the indicated transcripts were determined by real-time quantitative RT-PCR and expressed relative to the vehicle values at time 1 hour. Data are means ± SE of two independent experiments involving a total of 5 mice per condition. *(B)* Whole tissue extracts analyzed by immunoblotting for cleaved caspase-3, Bcl-2 and Bcl-xL. Equal loading was monitored by probing the blots for HSP90. Results are representative of 2 mice per condition and time point.

Supp Fig 11. The metalloproteinase inhibitor GM001 suppresses D-Gal/LPS-induced plasma TNF-α appearance in mice. CD1 mice were pretreated with GM6001 at the indicated doses or with vehicle (4% carboxymethylcellulose in water) and 40 min after injected i.p. D-galactosamine (740 mg/kg) plus lipopolysaccharides from E coli O111:B4 (37 μg/kg) (D-Gal/LPS). Plasma levels of TNF-α were assessed 60 min later using an ELISA kit. Plotted are individual plasma TNF-α levels from 2 independent experiments, with horizontal lines representing means.

Supp Fig 12. The broad-spectrum metalloproteinase inhibitor GM6001 does not prevent the acute induction of ErbB ligand and IEG transcripts by GLP-2 and EGF in mouse jejunum. CD1 mice were pretreated with GM6001 (150 mg/kg, i.p.) or vehicle (4% carboxymethylcellulose in water) and 40 min after injected with GLP-2 (0.2 mg/kg), EGF (1 mg/kg) or vehicle alone (PBS). Jejunum samples were collected 45 min later, total RNA was isolated and the levels of

the indicated transcripts determined by real-time quantitative RT-PCR analysis. Data, expressed relative to the values of vehicle alone-treated mice, are means ± SE of two independent experiments involving a total of 4 and 6 mice per condition, respectively, in the vehicle- and GM6001-pretreated groups. Two-way ANOVA revealed no interaction between pretreatment (vehicle, GM6001) and treatment (vehicle, GLP-2, EGF) for any of the transcripts. ** $p<0.01$ *vs* the same treatment within the vehicle-pretreated group.

Supp Fig 13. The small intestinal growth response to GLP-2 is preserved in *waved-2* mice. Relative small intestinal weight and length and jejunal histomorphometry in 11 weeks old littermate female mice of the specified *Egfr* genotype administered either native human GLP-2, h[Gly2]GLP-2 or vehicle alone (PBS) at the dose, schedule and for the number of days indicated. Villus height and crypt depth were assessed on histological jejunal transverse cross sections stained with H&E. Data are means ± SE of two independent experiments (n= 3 mice per genotype and condition). * $p<0.05$, ** $p<0.01$ and *** $p<0.001$ *vs* the corresponding vehicle-treated group.

Supp Fig 14. Pan-ErbB receptor activity is required for GLP-2-induced murine colonic growth. Relative colon weight and length and histomorphometry in CD1 mice pretreated with vehicle (water) or CI-1033 (30 mg/kg) 30 min prior to administration of h[Gly2]GLP-2 (0.2 mg/kg), EGF (0.4 mg/kg), KGF (2 mg/kg) or vehicle alone (PBS) once a day for 9 days. Crypt depth was assessed on transverse cross sections of the colon stained with H&E. Data are means ± SE of two independent experiments (5-6 mice per condition). * $p<0.05$, ** $p<0.01$ and *** $p<0.001$ *vs* the corresponding vehicle-treated group; + $p<0.05$ and ++ $p<0.01$ *vs* the same treatment within the vehicle-pretreated group.